1988

Shocks in the internal tide on the Australian North West Shelf

Adrian Hall Pincombe
University of Wollongong

SHOCKS IN THE INTERNAL TIDE ON THE AUSTRALIAN NORTH WEST SHELF

A thesis submitted in partial fulfilment
of the requirements for the award of the degree

MASTER OF SCIENCE (HONOURS)

from

THE UNIVERSITY OF WOLLONGONG

by

Adrian Hall Pincombe B.Sc.,Dip.Ed.

Mathematics
1988

ACKNOWLEDGEMENTS

I wish to thank my supervisor, Dr. N. F. Smyth, for his suggestion of the problem which is studied in this thesis and for his expert guidance and support throughout this study. Working with him has been an enjoyable and rewarding experience.

I would also like to thank Dr. C. Coleman for his helpful suggestions concerning numerical methods and convergence problems.

Thanks are also due to the Joint Venture Participants and the management of Woodside Offshore Petroleum Pty. Ltd. for the use of their Time Series observations of temperatures and currents. The Participants in the Domestic Gas Phase of the North West Shelf Venture are Woodside Petroleum Ltd.,BP developments Australia Ltd., California Asiatic Oil Co., Shell Development (Australia) Pty. Ltd. and BHP Petroleum Pty. Ltd. The data was collected by Steedman Ltd.

ABSTRACT

The evolution of shocks in the semi-diurnal internal tide on the Australian North West Shelf has previously been studied and an analytic solution has been found in terms of non-physical variables. Conversion of the results to physical variables requires the solution of the modal equation which can be solved analytically only if the background velocity profile is linear or constant. In this study the modal equation is solved numerically and this solution is used to study the effect of nonlinear background velocity profiles. It is found that profiles which are compatible with the profile of averaged currents can explain the observed shock heights as long as there is a strong shear near the surface. It is assumed that the strong current near the seabed, which is out of phase with the tide, can act as a background current and its effect is assessed. It is found that shocks which evolve under the influence of this current are upward hydraulic jumps, while the observed shocks are downward hydraulic jumps, but that a combination of this current with the background current profile considered above can still explain the observed shocks as long as the current near the seabed is only active within a limited height above the seabed. It is found that the slope of the background velocity profile is a critical factor in determining the breaking distance and the shock height and that large shears are required if the observed shock heights are to be attained. It is also shown that a smaller slope is required if the shear acts over a greater fraction of the depth and that when the current is against the tide the shears required to produce the shocks are smaller than they would be if the background current was in the direction of the tide.

TABLE OF CONTENTS

LIST OF TABLES

LIST OF FIGURES

1. Introduction

The Australian North West Shelf is a continental shelf off the northern coast of Western Australia and is an important oil and gas production area.It is characterised by strong tidal flows and by strong semi-diurnal internal tides (Holloway,1987). The interaction of the incoming tide with the shelf break causes a strong internal tide (amplitude ~ 30m). As the internal tide propagates shoreward it evolves under the influence of the background current and the shoaling of the bottom. There is a strong current flow, part of the large scale Leeuwin Current system, along the Western Australian coast which provides the background current for the evolution of the internal tide (Holloway and Nye,1985). Time series of the internal tide have been made at two locations; the first of these, located on the slope, near the shelf break, was at North Rankin and the second, located further onshore on the shelf proper, is known as Mooring 5. Holloway (1987) studied these observations of the evolution of the semi-diurnal internal tide and found some significant features. These features were not evident in the alongshore component of the internal tide so we consider the onshore component only. The bathymetry of the North West Shelf and the locations of North Rankin and Mooring 5 are shown in figure 1.1. Time series of isotherm heights and the onshore component of the current at various depths are shown in figure 1.2. The isotherms at North Rankin clearly show that hydraulic jumps (shocks) form in the tidal waveform. These shocks evolve under the influence of the background current and the changing depth. The tidal waveform at Mooring 5 is more complex. In each period the shock at North Rankin

(and the first shock at Mooring 5) is followed by high frequency waves (period ~ 20 minutes).

Holloway(1987) used a two layer internal hydraulic jump model and showed that when the flow near the surface became hydraulically supercritical, a downward hydraulic jump would occur, while a supercritical flow near the seabed gave an upward hydraulic jump. The two layer model gave approximate values of the jump heights within 20% of the observed values. Holloway also used the soliton solution of the Korteweg-de Vries equation to approximate the high frequency waves which follow the shocks at North Rankin and the first shock of each period at Mooring 5. He found that second order corrections to the Korteweg-de Vries equation were required before the periods and amplitudes agreed with the observed values.

Smyth and Holloway (1988) utilised the work of Grimshaw (1984) and the perturbation theory of Gear and Grimshaw (1983) which gave the second order corrections to the Korteweg-de Vries equation, and showed that, due to the long wavelength and small amplitude of the semi-diurnal internal tide, the propagation of the internal tide on the North West Shelf could be described, after scaling, by the perturbed extended Korteweg-de Vries equation

$$u_t + 6uu_x - \gamma(t)u^2u_x + \varepsilon u_{xxx} - \varepsilon\theta(t)uu_{xxx} = \sigma(t)u \qquad (1.1)$$

where the parameters $\gamma,\varepsilon,\theta$ and σ are defined in section 2. The coordinates x and t in this equation are not physical space and time; x is related to the physical phase variable and t is related to the physical space coordinate. The parameters γ and θ are of third order in amplitude. The third order terms are neccessary in order

to fully describe the observed flow. The perturbation term $\sigma(t)u$ is due to the shoaling of the bottom topography. The variable u is related to the physical displacement. Smyth and Holloway found that the parameter ε was $O(10^{-4})$ on the North West Shelf and hence that dispersive effects were weak, and the flow hydraulic, except in the region of a shock, where the derivatives of u are large. They solved the hydraulic form of equation (1.1)

$$u_t + 6uu_x - \gamma(t)u^2u_x = \sigma(t)u \qquad (1.2)$$

(since ε is small) and found that two shocks form in each period of the tide. In the neighbourhood of a shock where the dispersive terms cannot be neglected, Smyth and Holloway obtained a first order boundary layer solution to the full perturbed extended Korteweg-de Vries equation and showed that the first shock in each period breaks up into an undular bore, with the leading waves in the bore being close to solitons. They found that the second shock cannot break up into an undular bore.

In order to convert the results from (1.1) and (1.2) into physical variables, the modal equation

$$[\rho_0 (c_0 - v)^2 \phi_z]_z + \rho_0 N^2 \phi = 0 \qquad (1.3)$$

with $\phi(z) = 0$ at $z = 0$

$\phi(z) = \kappa(c_0 - v)^2 \phi_z(z)$ at $z=-h$

must be solved. This equation and its parameter κ are defined in section 2. The variables ρ_0 and v are the background density and current respectively and c_0 is the linear phasespeed. The modal equation has an analytical solution for v linear or constant (Gear and Grimshaw,1983). Smyth and Holloway showed that in the

absence of a background current, ie v=0, the semi-diurnal internal tide would not break as it propagated up the shelf. They also considered a linear shear current and found that the theoretical jump heights and breaking distances were in agreement with the observations for Richardson numbers (shears) near the observed values.

The actual background current on the North West Shelf is more complicated than a linear shear, with 24-hour averages of current, which were calculated by Holloway(1987), indicating a distinctly nonlinear background velocity profile (see figure 1.3). In the present work a numerical solution of the modal equation (1.3) will be used to make first order (in amplitude) calculations of the jump heights in terms of physical variables for nonlinear background current profiles. It will be shown that profiles which are compatible with the average currents of Holloway give shock heights in agreement with the observations. It is found that strong shears near the surface are required to give jump heights in accord with the observed values.

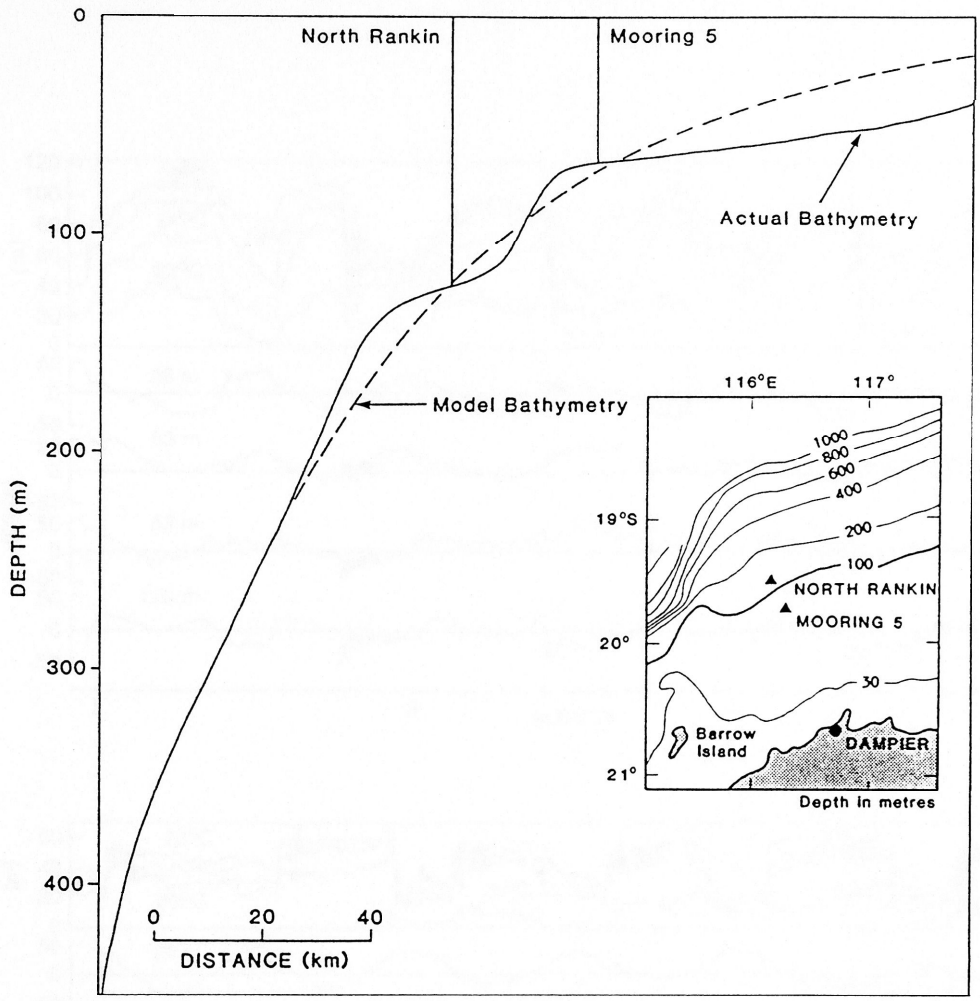

figure 1.1
shelf bathymetry showing locations
of North Rankin and Mooring 5

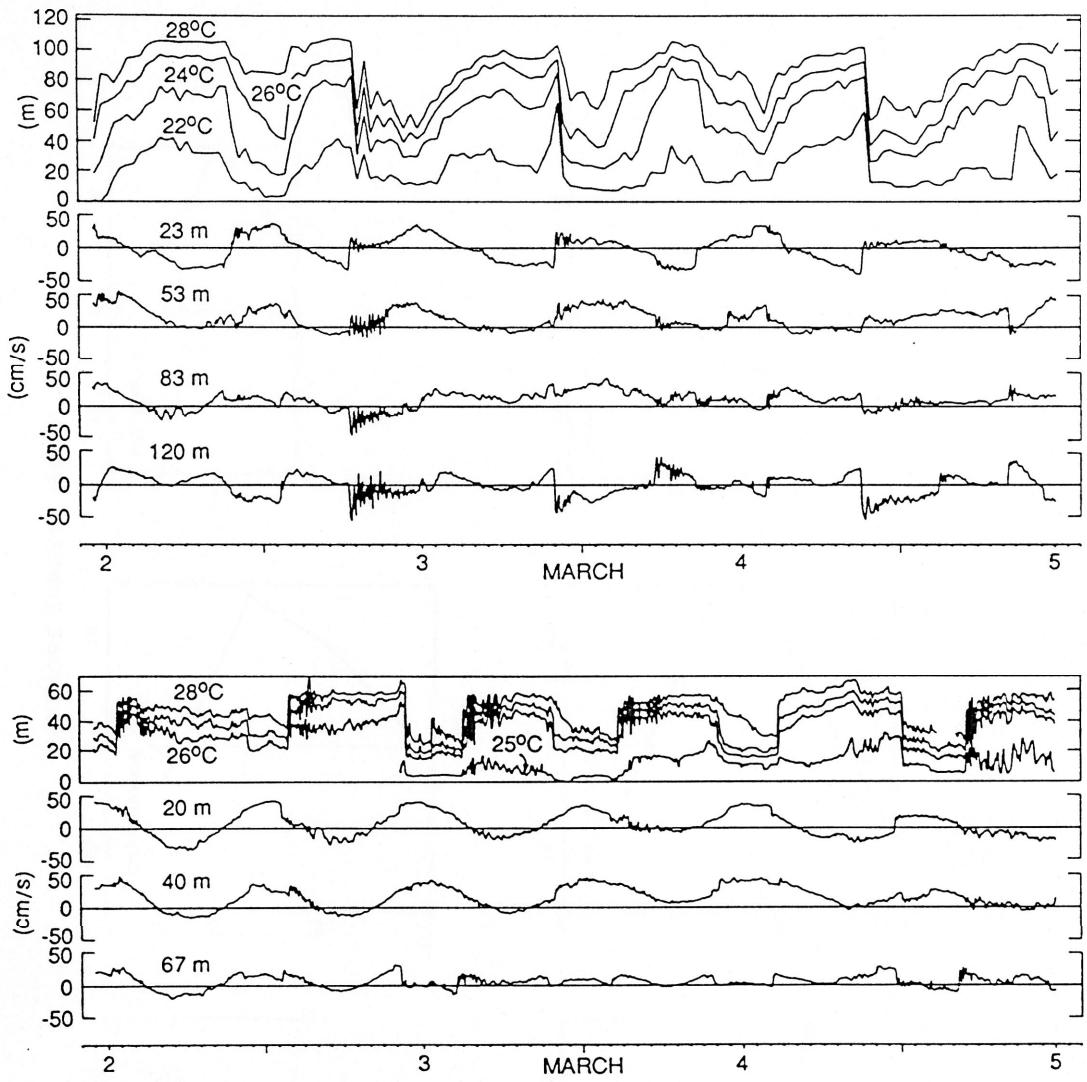

figure 1.2
time series of isotherms and currents
at North Rankin and Mooring 5

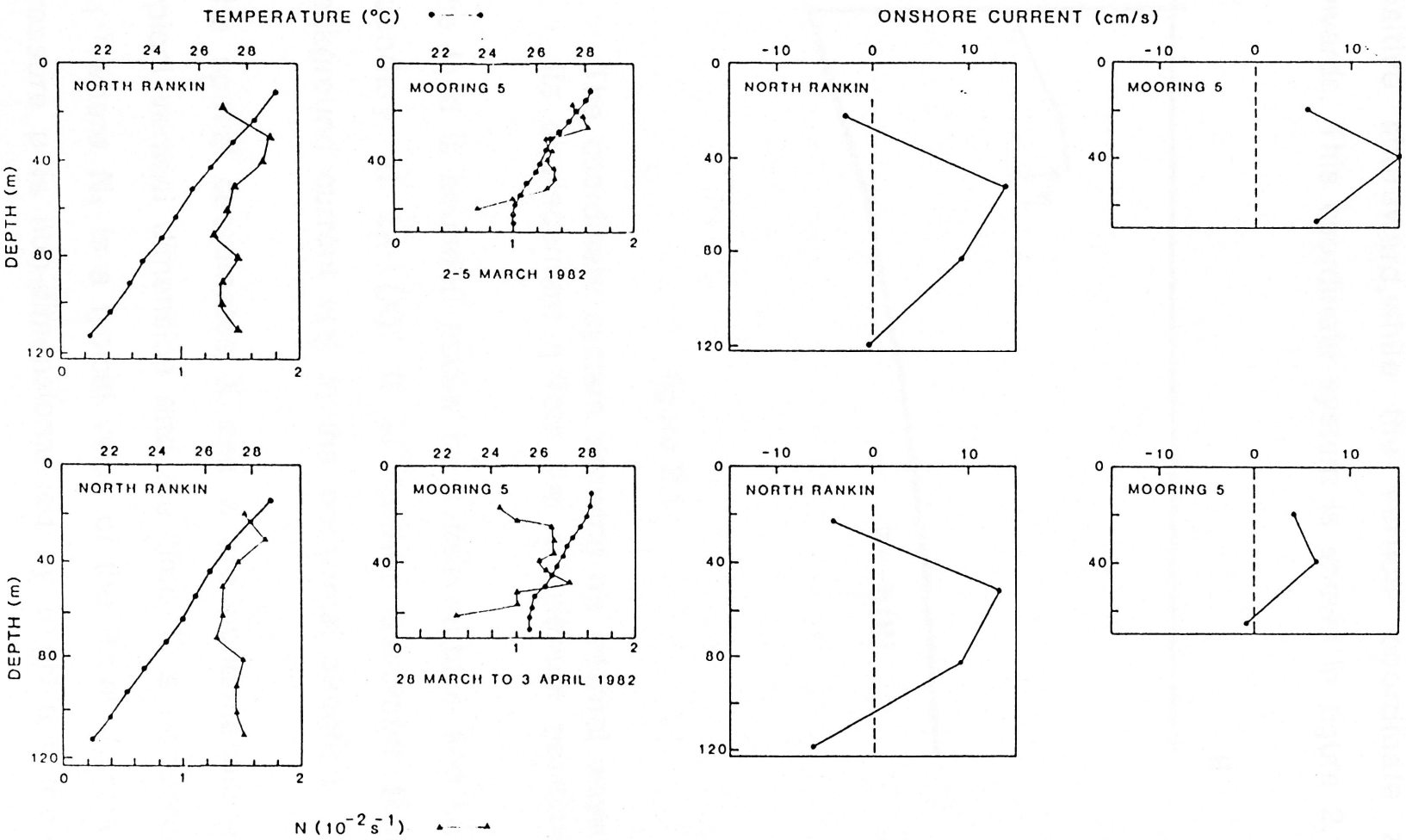

figure 1.3
24-hour averages of temperature
and current vs. depth

2. Development of equations governing semi-diurnal internal tide

Consider the two-dimensional flow of a stratified, inviscid incompressible fluid. The horizontal coordinate X is defined as positive shoreward,while the vertical coordinate z is positive upwards. This coordinate system is shown in figure 2.1.

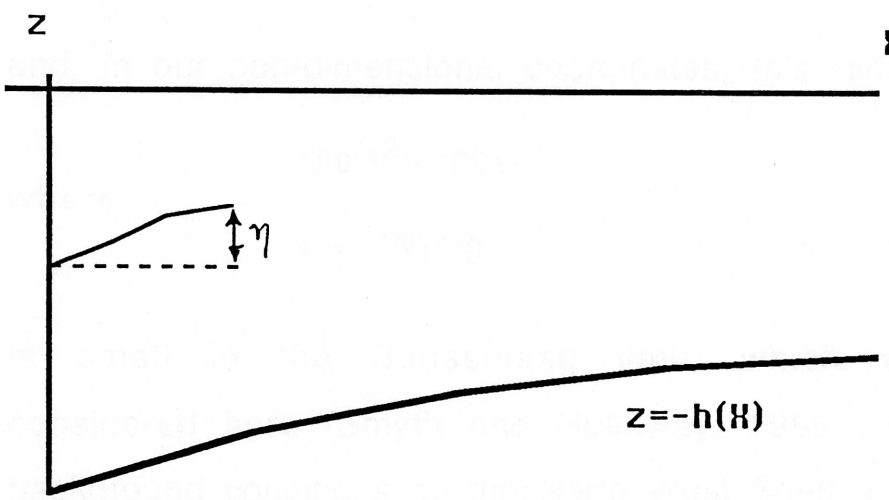

figure 2.1

The coordinate system showing an internal wave and its displacement η from the equilibrium position.

The fluid is bounded above by a free surface and below by a rigid boundary at z=-h(X). It is further assumed that there is a background current v(z) in the horizontal direction.

The spatial coordinates X and z are nondimensionalised by H, a typical vertical dimension and the time T is nondimensionalised by N_1^{-1},where N_1 is a typical value of the Brunt Vaisala frequency.The pressure p is non-dimensionalised by $\rho_1 gH$ and the density by ρ_1, where ρ_1 is a typical density. Under these circumstances, the z

derivative of the undisturbed (background) pressure p_0 is

$$p_{0z} = -\rho_0 \tag{2.1}$$

where ρ_0 is the non-dimensionalised undisturbed (background) density. The Brunt-Vaisala frequency is defined by

$$N^2 = -\frac{\rho_{0z}}{\rho_0} \tag{2.2}$$

and, in our non-dimensional coordinates, this reduces to

$$\kappa\rho_0 N^2 = -\rho_{0z} \tag{2.3}$$

where

$$\kappa = HN_1^2/g \tag{2.4}$$

is small in the Boussinesq limit, which will be the limit considered here (Smyth and Holloway, 1988 , found that for the background conditions on the North West Shelf, $\kappa \sim 0.0025$).

There is a horizontal background current v flowing from left to right, the magnitude of which can vary with depth. The fluid is assumed to be stratified so that $\rho_0 = \rho_0(z)$. If the background flow is perturbed, lines of constant density are vertically displaced from their equilibrium positions. We denote this vertical displacement by η, and the density at some depth z is then given by $\rho_0(z-\eta)$.

The equations of motion in our two dimensional case are

$$u_x + w_z = 0 \tag{2.5}$$

$$\rho_0(z-\eta)\frac{du}{dT} + q_x + \rho_0(z-\eta)w\frac{dv}{dz} = 0 \tag{2.6}$$

$$\rho_0(z-\eta)\frac{dw}{dT} + q_z + \frac{1}{\kappa}\{\rho_0(z-h) - \rho_0(z)\} = 0 \qquad (2.7)$$

$$w = \frac{d\eta}{dT} \qquad (2.8)$$

where $\frac{d}{dT} = \frac{\partial}{\partial T} + (v+u)\frac{\partial}{\partial X} + w\frac{\partial}{\partial z}$,

u and w are horizontal and vertical velocities relative to the background state, and κq is the pressure relative to the background state. We assume that the waves are of small amplitude and long wavelength so that the small parameters

$$\alpha = \frac{a}{H}$$

and (2.9)

$$\beta = \frac{H}{L}$$

can be defined. Here a is a typical wave amplitude and L is a typical lengthscale (wavelength) of the wave.

In order to study the evolution of the semi-diurnal internal tide we define slow space and time variables

$$\chi = \beta X \qquad \text{and} \qquad \lambda = \beta T \qquad (2.10)$$

and then look for a solution of the form

$$\eta = \alpha\eta_0(\chi,\lambda,z) + \alpha^2\eta_1(\chi,\lambda,z) + O(\alpha^3)$$

$$q = \frac{p}{\kappa} = \alpha q_0(\chi,\lambda,z) + \alpha^2 q_1(\chi,\lambda,z) + O(\alpha^3) \qquad (2.11)$$

$$u = \alpha u_0(\chi,\lambda,z) + \alpha^2 u_1(\chi,\lambda,z) + O(\alpha^3)$$

since we expect η,q and u to all be $O(\alpha)$. Using these expansions we can simplify the equations of motion by separating them into

effects of various orders of magnitude.

First order equations

When the expansions (2.11) are substituted into equations (2.5) to (2.8), the equations separate into groups of terms of order α,α^2,α^3,etc and into groups of order $\beta\alpha,\beta\alpha^2,\beta\alpha^3$,etc. There is one group of terms however which has orders $\beta^2\alpha^2,\beta^2\alpha^3$,etc. We can incorporate these terms into the first order equations or into the equations of any higher order by choice of a new parameter ε. Here we choose $\varepsilon = \beta^2/\alpha$, placing the first of these terms in the equations of second order, on assuming ε is O(1). The parameter ε is an inverse Ursell number. We will see later that this choice determines the complexity of the eventual equation describing the χ,λ dependence of the internal wave. In this case the first order equations are

$$u_0\,\chi + w_0\,z = 0$$

$$\rho_0 \frac{Du_0}{D\lambda} + q_0\chi + w_0 \frac{dv}{dz} = 0$$

$$q_0\,z + \rho_0 N^2 \eta_0 = 0 \qquad (2.12)$$

$$w_0 = \frac{D\eta_0}{D\lambda}$$

where $$\frac{D}{D\lambda} = \frac{\partial}{\partial\lambda} + v\frac{\partial}{\partial\chi}$$

subject to $$\eta_0 = 0 \text{ at } z=-h$$

$$\kappa q_0 = \rho_0\eta_0 \text{ at } z=0 \qquad (2.13)$$

A process of differentiation and substitution applied to equations (2.12) condenses them into a single equation in η,

$$[\rho_0(\eta_{0\,\lambda\lambda z} + 2\eta_{0\,\lambda\chi z} + v^2\eta_{0\,\chi\chi z})]_z + \rho_0 N^2 \eta_{0\,\chi\chi} = 0 \qquad (2.14)$$

The internal waves propagate in the X direction, so we seek to separate variables by looking for a travelling wave solution of the form $\eta_0 = A_n(\chi - c_0\lambda)\phi_n(z)$. Then (2.14) reduces to

$$[\rho_0(c_{0\,n}-v)^2\phi_{n\,z}(z)]_z + \rho_0 N^2 \phi_n(z) = 0 \qquad (2.15)$$

subject to $\phi_n = 0$ at $z = -h$

$\phi_n = \kappa(c_{0\,n} - v)^2\,\phi_{n\,z}$ at $z=0$,

which is an eigenvalue problem determining the eigenvalues c_0, the linear phasespeed. The set of functions $\phi_{n\,z}(z)$ is orthogonal with a normalizing factor I_n where

$$I_n = 2\int_{-h}^{0} \rho_0(c_{0\,n}-v)\phi_n{}^2{}_z\,dz \qquad (2.16)$$

Since the ϕ_n form a complete orthogonal set, we may consider a single mode only. Let us then set

$$\begin{aligned} \eta_0 &= A(\chi,\lambda)\phi_{n\,z} \\ q_0 &= \rho_0(c_{0\,n}-v)^2 B(\chi,\lambda)\phi_{n\,z}(z) \qquad (2.17) \\ u_0 &= -(c_{0\,n}-v)E(\chi,\lambda)\phi_{n\,z}(z) - \eta_0 v_z \end{aligned}$$

Using the forms (2.17) we can substitute into (2.12) to obtain an equation for $A(\chi,\lambda)$. The resulting equation is

$$\frac{D^2A}{D\lambda^2} = (c_{0\,n}-v)^2 A_{\chi\chi}\,, \qquad (2.18)$$

which is the homogeneous one dimensional wave equation and it

can easily be seen that it places no restriction on $A(\chi,\lambda)$ other than that $A(\chi - c_{0\,n}\lambda)$ is a solution.

Higher order equations

By choosing appropriate forms for η_1, q_1 and u_1 we can solve the second order equations by the same method. The z dependence of these second order terms is defined by the same $\phi_n(z)$ functions which described the first order terms. The second order terms are naturally more complex and include terms which are quadratic in ϕ_n. At this order, the usual Korteweg-de Vries equation is obtained. However, to fully describe the evolution of the semi-diurnal internal tide, terms of $O(\alpha^3)$ must be included. An equation defining the χ,λ dependence can be derived from the second order equation including some third order terms and after some transformations we obtain

$$u_t + 6uu_x - \gamma(t)u^2u_x + \varepsilon u_{xxx} - \varepsilon\theta(t)u_{xxx} = \sigma(t)u \qquad (2.19)$$

This is the perturbed extended Korteweg-de Vries equation and the variables involved are non-physical. The relationships between x,t and the physical space and time variables X,T are given by

$$t = \int_0^{\alpha\beta X} \frac{dX'}{c_0(X')}$$

$$x = \frac{t - \alpha\beta T}{\delta^{1/3}\alpha} \qquad (2.20)$$

where c_0 is the linear phasespeed of the internal waves. The physical displacement of the wave,η, is related to u through the

equation

$$\eta = \frac{6\alpha\delta^{1/3}}{\mu} u\,\phi_n + \alpha^2\eta_1 + O(\alpha^3) \qquad (2.21)$$

The influence of the z coordinate has been integrated out to obtain equation (2.19) and the coefficients $\gamma(t),\theta(t),\sigma(t)$ are defined in terms of integrals over the range of z values (-h,0). All three of $\gamma(t)$, $\theta(t)$, $\sigma(t)$ can be defined in terms of I,μ,δ and t, while μ and δ also appear in the definitions of x,(2.20), and η,(2.21). The variable I is simply the normalizing factor I_n defined in equation (2.16) and the variables μ and δ are defined by

$$\begin{aligned} c_0 I\mu &= 3\int_{-h}^{0} \rho_0 (c_0-v)^2 \phi_{nz}{}^3\, dz \\ c_0{}^3 I\delta &= \int_{-h}^{0} \rho_0 (c_0-v)^2 \phi_n{}^2\, dz \end{aligned} \qquad (2.22)$$

The term $\sigma(t)u$ is a perturbation term and is the effect of the shoaling of the seabed. The parameter $\sigma(t)$ is defined by

$$\sigma(t) = \frac{-(c_0{}^2 I)_t}{2c_0{}^2 I} - \frac{\mu}{\delta^{1/3}}(\delta^{1/3}/\mu)_t \qquad (2.23)$$

The higher order term $\gamma(t)u^2u_x$ is a nonlinear term which is third order in the amplitude α. Smyth and Holloway (1988) showed that this term is the source of the second shock in each period at Mooring 5. The parameter $\gamma(t)$ is defined by

$$\gamma(t) = \frac{72\alpha\delta^{1/3}\sigma_2}{\mu} + \frac{108\alpha\sigma_3\delta^{1/3}}{\mu^2} \qquad (2.24)$$

where σ_2 and σ_3 are both defined by integrals with respect to z where the integrand in each case is extremely complex. They are not defined here because they are not used in this study.

The terms involving ε in (2.19) are dispersive terms with $\varepsilon=\beta^2/\alpha$ as before and the parameter $\theta(t)$ defined by

$$\theta(t) = \frac{12\alpha\sigma_2\delta^{1/3}}{\mu} \qquad (2.25)$$

Smyth and Holloway (1988) showed that $\varepsilon \sim O(10^{-4})$ so that the dispersive terms are small except when u_{xxx} becomes large. This occurs in the vicinity of a shock. In the first order treatment of shock formation which is being undertaken here, we can neglect these terms.

We have seen that the wave motion can be described by a combination of two equations. We need to solve equation (2.19) for u(x,t) where u,x and t are all nonphysical variables. In order to transform these nonphysical variables into the physical space,time and wave displacement variables X,T and η we must solve equation (2.15) for $\phi(z)$ and c_0 and use these results to calculate $I,\mu,\delta,\sigma(t),\gamma(t)$ and $\theta(t)$.

3. The Numerical Solution

We can obtain a first order estimate of the solution by solving the reduced equation

$$u_t + 6uu_x = \sigma(t)u \qquad (3.1)$$

Equation (3.1) is the shallow water equations to second order in amplitude and can be solved by the method of characteristics . In characteristic form

$$\frac{du}{dt} = \sigma(t)u \qquad (3.2)$$

on $$\frac{dx}{dt} = 6u \qquad (3.3)$$

These equations have the solution

$$u = f(\xi)\, e^{\int_0^t \sigma(\tau)d\tau} \qquad (3.4)$$

on the characteristics

$$x = 6f(\xi) \int_0^t e^{\int_o^\theta \sigma(\tau)d\tau} d\theta + \xi \qquad (3.5)$$

where $x = \xi$, $u = f(\xi)$ when $t = 0$

As we saw in section 2 , the value of u in (3.1) is not a direct representation of wave displacement but is related to physical displacement by (2.21). However , changes in u and changes in physical displacement correspond . It can be seen from (3.2) that

wave speed is proportional to the amplitude u so that a positive wave (u>0) will eventually form a shock . This will happen regardless of whether the physical wave is positive ($\eta>0$) or negative ($\eta<0$). By converting (3.1) to conservation form we find the shock velocity is

$$U = 3(u_1 + u_2) \qquad (3.6)$$

where u_1 and u_2 denote the value of u just ahead of and just behind the shock respectively.

Smyth and Holloway (1988) solved (3.1) for u in terms of the non-physical variables x,t but ,before shock heights and physical variables could be calculated , the modal equation (2.15) had to be solved for $\phi(z)$ and c_0. The following solution method follows Smyth and Holloway (1988).

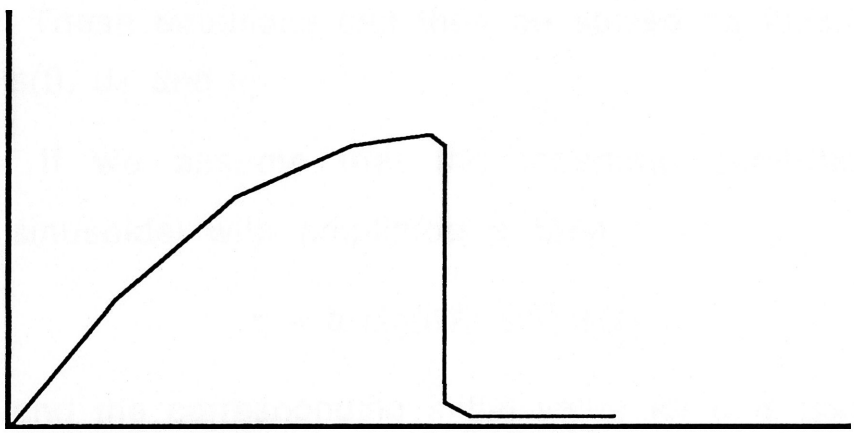

figure 3.1
A shock in a u wave
$\xi=\xi_2$ behind the shock $\xi=\xi_1$ ahead of the shock

If s(t) denotes the position of the shock (see figure 3.1) then we can use the fact that the characteristics cross at the shock to obtain the following pair of simultaneous equations

$$s(t) = 6f(\xi_1)\int_0^t e^{\int_0^\theta \sigma(\tau)d\tau} d\theta + \xi_1 \qquad (3.6)$$

$$s(t) = 6f(\xi_2)\int_0^t e^{\int_0^\theta \sigma(\tau)d\tau} d\theta + \xi_2 \qquad (3.7)$$

A third simultaneous equation comes from the conservation relation

$$\int_{\xi_2}^{\xi_1} f(\xi)d\xi = \frac{1}{2}(\xi_1 - \xi_2)(f(\xi_1) + f(\xi_2)) \qquad (3.8)$$

These equations can then be solved as follows to eventually obtain s(t), u_1 and u_2 .

If we assume that the incoming semi-diurnal internal tide is sinusoidal with amplitude a then

$$\eta = a \sin(KX - \omega T)\, \phi(z) \qquad (3.9)$$

and the corresponding initial value for u is given by

$$f(\xi) = A \sin(B\xi) \qquad (3.10)$$

where A,B are constants .

At the initial point , t=0 ,X=0 ,$x = -\frac{\beta}{\delta^{1/3}}T$ and $x = \xi$ giving the relation

$$T = -\frac{\delta^{1/3}}{\beta}\,\xi \qquad (3.11)$$

It follows from (2.20) that

$$B = -\frac{\delta_0^{1/3}\omega}{\beta} \qquad (3.12)$$

and

$$A = \frac{\mu_0 a}{6\alpha\delta_0^{1/3}} \qquad (3.13)$$

where δ_0 and μ_0 are the initial values of δ and μ respectively. By substuting for $f(\xi)$ from (3.10) into (3.6) to (3.8) we can solve these equations for shock height and position . For the initial condition (3.10) , it can be shown that (3.6) to (3.8) can be reduced to three simpler equations

$$\xi_1 + \xi_2 = \frac{2\pi}{B} \qquad (3.14)$$

$$s(t) = \frac{\pi}{B} \qquad (3.15)$$

and

$$\int_0^t e^{\int_0^\theta \sigma(\tau)d\tau} d\theta = \frac{\psi}{6AB \sin \psi} \qquad (3.16)$$

where ψ is defined by $\xi_1 - \xi_2 = \frac{2\psi}{B}$

Note that (3.15) shows that the location of the shock in terms of the nonphysical coordinate x is constant . This is not true for physical variables .

When the shock is first formed $\xi_1 = \xi_2$ (ie $\psi = 0$) so that the position at which the wave first breaks is given by the X value for which

$$I_2 = \frac{1}{6AB} \qquad (3.17)$$

where $$I_2 = \int_0^t e^{\int_0^\theta \sigma(\tau)d\tau} d\theta \qquad (3.18)$$

The nonphysical shock strength $u_1 - u_2$ can be calculated from (3.4) as

$$u_1 - u_2 = I_3 \, (f(\xi_1) - f(\xi_2)) \qquad (3.19)$$

where

$$I_3 = e^{\int_0^t \sigma(\tau)d\tau} \qquad (3.20)$$

giving

$$u_1 - u_2 = 2AI_3 \sin \psi \qquad (3.21)$$

At this stage (3.1) has been solved, but in order to evaluate the physical shock strength we have to use (2.23) to express $\sigma(t)$ in terms of c_0, μ, δ, I and t and to evaluate the integral I_3. The variables c_0, μ, δ, I are obtained by solving the modal equation (2.15) for c_0 and $\phi(z)$ and then solving the integrals (2.16) and (2.22) to obtain μ, δ, I. Hence the expression (2.21) for η gives

$$\eta_1 - \eta_2 = 2a \frac{\mu_0 \delta^{1/3}}{\mu \delta_0^{1/3}} I_3 \sin(\psi) \, \phi(z) \qquad (3.22)$$

It is the maximum value of this shock strength (ie $\phi(z)=1$) which will be compared with the observations of Holloway(1987). To calculate the shock height as a function of t , ψ is found as a function of t from (3.16). Relating X to t through (2.20) then gives the shock height as a function of the nondimensionalised distance up the shelf X.

The modal equation can be solved analytically only for v linear or constant but the background velocity profile shown in figure 1. 3 is distinctly nonlinear , so (3.21) and (3,22) must be solved numerically. It is this numerical implementation which will now be discussed

Discretisation

Both the z and X coordinates are scaled using a typical depth (110 m.) and then some maximum scaled X is chosen. For most of this analysis, X_{max} = 800 was used giving a study boundary well beyond the region of interest. The furthest inshore observation point, Mooring 5, is at X = 510.

A number of steps is chosen for each direction (say m steps in the z direction and I steps in the X direction). The discrete values of X are then X_i , 1<=i<= I+1 and the corresponding depths h_i are calculated using the model bathymetry developed by Smyth and Holloway (1988) (see figure 1.1).

$$h_i = 2 \exp(-KX) \qquad (3.23)$$

where $K=2.2x10^{-3}$.

The model bathymetry and the actual bathymetry are shown in figure 1.1.

Because depth varies with X, a different vertical stepsize Δz_i must be calculated for each X_i , allowing the calculation of m+1 discrete values of z for each X_i. If we call these z values z_{ij} , $1 \leq j \leq m+1$, then values of density are given by

$$\rho_{ij} = \exp(-2.5x10^{-3} z_{ij}) \qquad (3.24)$$

on using an exponential background density $\rho=\exp(-\kappa z)$ and noting that $\kappa=2.5\times10^{-3}$(Smyth and Holloway,1988).

The background velocity v(z) is a known function of z and is represented by $v_{ij} = v(z_{ij})$.

Numerical form of eigenvalue equation

Differential equations of the form

$$[p(z)\,\phi_z(z)]_z + q(z)\,\phi(z) = 0 \qquad (3.25)$$

can be solved numerically using the discretization

$$\frac{1}{\Delta z}\left(p_{n+1/2}\left(\frac{\phi_{n+1}-\phi_n}{\Delta z}\right) - p_{n-1/2}\left(\frac{\phi_n-\phi_{n-1}}{\Delta z}\right)\right) + q_n\,\phi_n = 0 \qquad (3.26)$$

for $0 < n < m$

The expression (3.26) defines a system of m-1 equations in m-1 variables where ϕ_0 and ϕ_m are given by the boundary conditions (see (2.15)). This scheme is second order accurate and comes from approximating the derivatives by centred differences. In this analysis, since κ is small in (2.15) we use the boundary conditions $\phi_0=\phi_m=0$ and the discretized form of the problem is thus

$$\begin{aligned}
&(\Delta z^2 q_1 - p_{3/2} - p_{1/2})\,\phi_1 + p_{3/2}\,\phi_2 = 0 \\
&p_{n-1/2}\,\phi_{n-1} + (\Delta z^2 q_n - p_{n+1/2} - p_{n-1/2})\,\phi_n + p_{n+1/2}\,\phi_{n+1} = 0 \\
&p_{m-1/2}\,\phi_{m-1} + (\Delta z^2\,\phi_m - p_{m+1/2} - p_{m-1/2})\,\phi_m = 0
\end{aligned} \qquad (3.27)$$

for $1<n<m$

This can be expressed in matrix form as

$$A\underline{\phi} = 0 \qquad (3.28)$$

where A is a tri-diagonal (m-1)x(m-1) matrix. The eigenvalue c_0 is determined by the condition that the matrix be singular so that the system of equations has a solution.

Calculation of c_0

The eigenvalue equation (2.15) has an infinite number of solutions but we only require a mode 1 solution since the incoming tide is a mode 1 wave. In (3.28) p is a function of c_0 and z and the problem is to find the largest value of c_0 which satisfies $A\phi=0$. This c_0 is the largest value for which

$$\det(A) = 0 \qquad (3.29)$$

To find approximate values of c_0 , the secant method is used. D=det(A) is calculated for two values of c_0,

$$c_{0\,1} \quad \text{---}> \quad D_1$$
$$c_{0\,2} \quad \text{---}> \quad D_2$$

The derivative of the function D=det(A) is then approximated by

$$D' = \frac{D_2 - D_1}{c_{0\,2} - c_{0\,1}} \qquad (3.30)$$

and the new value of c_0 is calculated using

$$c_{0\,3} = c_{0\,2} - \frac{D_2}{D'} \qquad (3.31)$$

The determinant is calculated by reducing the original tri-diagonal matrix to an upper triangular matrix A'. This reduction is achieved using the fact that the determinant is unchanged if a multiple of one row is subtracted from another row. This gives

$$\det(A) = \text{trace}(A') \tag{3.32}$$

These steps are undertaken iteratively using

$$D' = \frac{D_n - D_{n-1}}{c_{0\,n} - c_{0\,n-1}}$$

$$c_{0\,n+1} = c_{0\,n} - \frac{D_n}{D'} \tag{3.33}$$

until convergence is achieved.

Calculation of $\phi(z)$

Once we have obtained the first eigenvalue c_0, we need to solve (3.28) for the corresponding eigenvector $\phi=\{\phi_i\}$. This is not straightforward because A is singular and $\phi(z) \equiv 0$ is a possible solution. The eigenvector is found by the conjugate gradient method (see Kammerer and Nashed , 1972). An initial vector ϕ_0 is chosen and

$$r_0 = s_0 = A^t A \phi_0 \tag{3.34}$$

is computed, where A^t is the transpose of A. Then

$$\alpha_0 = \langle r_0, r_0 \rangle \,/\, \langle As_0, As_0 \rangle \tag{3.35}$$

and

$$\phi_1 = \phi_0 - \alpha_0 s_0$$

are calculated , where $\langle x,y \rangle = x_1y_1+x_2y_2+.....$

Then the following calculations are done iteratively until the solution converges.

$$r_i = r_{i-1} - \alpha_{i-1} A^t A s_{i-1} \tag{3.36}$$

$$\beta_{i-1} = - \langle r_i, A^t A s_{i-1} \rangle / \langle As_{i-1}, As_{i-1} \rangle \tag{3.37}$$

$$s_i = r_i - \beta_i s_{i-1} \tag{3.38}$$

$$\alpha_i = \langle r_i, s_i \rangle / \langle As_i, As_i \rangle \qquad (3.39)$$

$$\phi_{i+1} = \phi_i - \alpha_i s_i \qquad (3.40)$$

The test for convergence was made on the value of $\langle \alpha_i s_i, \alpha_i s_i \rangle$.

The integrals for $I, c_0 I_\mu$ and $c_0^3 I_\delta$

All three integrals (2.16) and (2.22) are approximated using Simpsons rule. The value of each function in the integrand needs to be established for each z_j (here we are integrating over z_{ij} for i=constant). All functions except ϕ_z have already been calculated numerically. The derivative ϕ_z is calculated using the second order accurate centred difference formula

$$\phi_{n\,z} = \frac{\phi_{n+1} - \phi_{n-1}}{2\Delta z} \qquad 1 < n < m+1 \qquad (3.41)$$

in the interior of the domain and the first order differences

$$\phi_{1\,z} = \frac{\phi_2 - \phi_1}{\Delta z}$$

$$\phi_{m+1\,z} = \frac{\phi_{m+1} - \phi_m}{\Delta z} \qquad (3.42)$$

at the end points.

Each of the integrals can be reduced to

$$G = \int_{-h}^{0} F dz \qquad (3.43)$$

where F is known at each of the nodes i=1 to m+1. Then G is approximated by

$$G=\frac{h}{6}\{F_1+F_{m+1}+4(F_2+F_4+F_6+.....)+2(F_3+F_5+.....)\} \quad (3.44)$$

The values of μ_i and δ_i can then be found in the obvious way.

Estimation of t

The shock height is found as a function of t from (3.30). To find this quantity as a function of the actual distance up the shelf, X needs to be determined in terms of t. The value of t is defined in terms of X by the indefinite integral (2.20) , so that discrete values of t are given by

$$t_i = \int_0^{\alpha\beta X_i} \frac{dX'}{c_0(x')} \quad (3.45)$$

in terms of X_i.

In order to evaluate this integral numerically, the eigenvalue problem has to be solved for a whole new range of distances

$$X'_i = \alpha\beta X_i \qquad 1<= i <= I+1 \qquad (3.46)$$

to find $c'_{0\,i} = c_0(X'_i)$.

The initial value of t_i is , by definition, $t_1=0$, and t_2 is estimated using the trapezoidal rule

$$t_2 = 0.5\left(\frac{1}{c'_{0\ 1}}+\frac{1}{c'_{0\ 2}}\right)\Delta X' \quad (3.47)$$

All subsequent values of t_i are calculated using a floating Simpson's formula defined by the recurrence relation

$$t_i = t_{i-2} + \left(\frac{1}{c'_{0\ i-2}} + \frac{4}{c'_{0\ i-1}} + \frac{1}{c'_{0\ i}}\right)\Delta X'/6 \qquad (3.48)$$

The integral $I_2(t)$

This function is defined by an indefinite integral and must be evaluated before we can solve (3.16) for ψ. Its discrete form is a vector $I_{2\ i}$ defined by

$$I_{2\ i} = \int_0^{t_i} y(\theta)d\theta \qquad (3.49)$$

The integral is over t and the step sizes Δt_i are variable as it is the steps ΔX_i which are of constant length. The value of the integrand is known at X_i and X_i is related to t_i by (3.45). Because of the variable step size, Simpson's rule can not be directly applied. A floating form of the trapezoidal rule could be used but the function I_2 is of critical importance in determining the shock strength. Because of this, a quadratic interpolation, as in Simpson's rule, is warranted.

Consider three points $(t_1,y_1),(t_2,y_2),(t_3,y_3)$. The coordinates may be shifted so that the points become $(-\Delta t_1,y_1),(0,y_2),(\Delta t_2,y_3)$. Then the value of the integral

$$\text{Area} = \int_{-\Delta t_1}^{\Delta t_2} y\,dt \qquad (3.50)$$

where

$$y=at^2 + bt + c \qquad (3.51)$$

is given by

$$\text{Area} = \frac{\Delta t_2+\Delta t_1}{6}\{2(y_1+y_2+y_3) - 2a\Delta t_1\Delta t_2 + b(\Delta t_2-\Delta t_1)\} \tag{3.52}$$

where

$$a = \frac{\Delta t_2(y_2-y_1) + \Delta t_1(y_3-y_2)}{\Delta t_1\Delta t_2(\Delta t_1 + \Delta t_2)}$$

and

$$b = \frac{\Delta t_1^2(y_3-y_2)-\Delta t_2^2(y_1-y_2)}{\Delta t_1\Delta t_2(\Delta t_1+\Delta t_2)}$$

The approximation method used for calculating $I_{2\,i}$ is analagous to the method used to calculate t_i. Substituting for $\sigma(t)$ from (2.23) we find that

$$\int_0^t \sigma(\tau)d\tau = \left[\ln\left(\frac{\mu}{\delta^{1/3}c_0 I^{1/2}}\right)\right]_{\tau=0}^{\tau=t} \tag{3.55}$$

The integrand y is then defined by

$$y = I_3 = \frac{\mu_i c_{0\,1}\,\delta_1^{1/3} I_1^{1/2}}{\mu_1 c_{0\,i}\,\delta_i^{1/3} I_i^{1/2}} \tag{3.56}$$

Then

$$I_{2\,1} = 0$$

$$I_{2\,2} = \frac{1}{2}(y_1+y_2)(t_2-t_1)$$

and, for i=3 to I+1,

$$I_{2\,i} = I_{2\,i-2} + \frac{t_i-t_{i-2}}{6}\{$$

$$2(y_i+y_{i-1}+y_{i-2})$$

$$-2a(t_{i-1}-t_{i-2})(t_i-t_{i-1})$$

$$+b(t_i-2t_{i-1}+t_{i-2}) \} \qquad (3.57)$$

Calculation of ψ

The function ψ is defined implicitly by equation (3.16) and for known values of $I_{2\,i}$ we can solve the following equation for ψ_i where i=1 to I+1.

$$\sin\psi_i - \frac{\psi_i}{6ABI_{2\,i}}=0 \qquad (3.58)$$

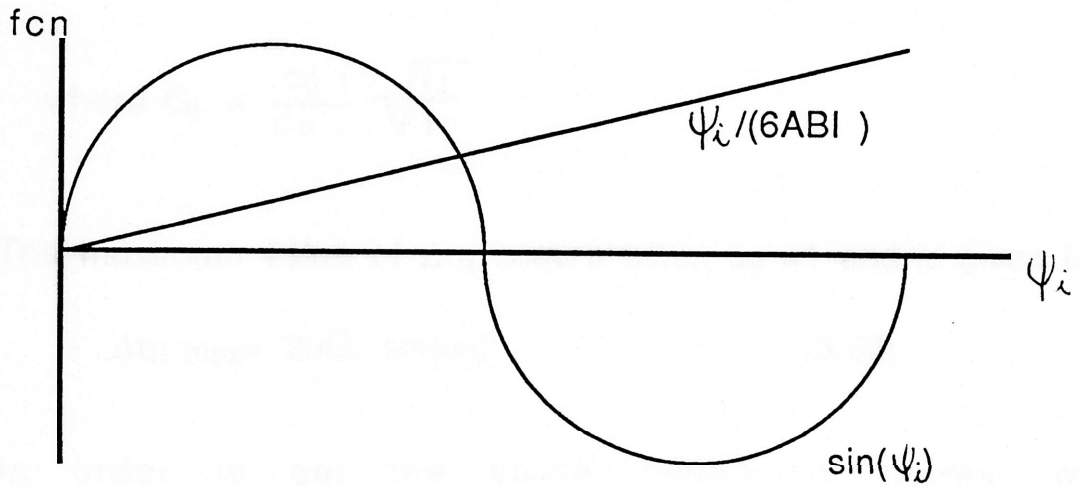

figure 3.2

simultaneous solution for ψ_i.

Equation (3.58) represents the simultaneous solution of $y=\sin\psi_i$ and $y=\frac{\psi_i}{6ABI_{2\,i}}$, as shown in figure 3.2. This solution may be found iteratively by Newtons method with

$$f(\psi_i) = \sin \psi_i - \frac{\psi_i}{6AB I_{2\,i}}$$

$$f'(\psi_i) = \cos \psi_i - \frac{1}{6AB I_{2\,i}} \qquad (3.59)$$

and

$$\psi_{i\ new} = \psi_{i\ old} - \frac{f(\psi_{i\ old})}{f'(\psi_{i\ old})}$$

Shock strength

The physical shock strength is defined by equation (3.20), where η_1-η_2 must now be calculated for each discrete value of X_i. If we call these shock strengths $\Delta\eta_i$, then

$$\Delta\eta_i = 2aG_i \sin \psi_i \ \phi_{ij} \qquad (3.60)$$

where $G_i = \frac{c_{0\,1}}{c_{0\,i}} \sqrt{\frac{I_1}{I_i}}$

The maximum value of $\Delta\eta_i$ occurs when ϕ_{ij} =1 and is given by

$$\Delta\eta_{i\ max} = 2aG_i \sin(\psi_i) \qquad (3.62)$$

In order to get the shock height in metres, we must redimensionalize (3.62) by multiplying it by the typical depth (110m.). This gives an estimation of the physical shock height

$$S = 110\ \Delta\eta_{i\ max} \qquad (3.63)$$

which we can compare with the observations.

Breaking distance

From (3.17) and (3.49), breaking distance is given by

$$I_{2\,i} = \frac{1}{6AB} \qquad (3.64)$$

The function $I_{2\,i}$ is known at discrete values of X only, so the breaking distance is found by a process of search and interpolation.

4. Validation of numerical solution

Analytical solution for linear shear

The case of a uniformly stratified fluid with a linear background velocity

$$v(z) = k(z+h) \qquad (4.1)$$

has been solved analytically for $k \leq 0$ (Gear and Grimshaw 1983,Smyth and Holloway 1988) and provides a non-trivial test case for the numerical model. Here the solution is generalised to include $k>0$. For a Boussinesq fluid the density varies slowly, ($\rho_z \sim O(10^{-3})$ or less for the background density profile on the North West Shelf) so that expressions containing ρ_z can be neglected in first order calculations. If we treat ρ as a constant, then (2.15) becomes

$$c_0^2[\ (1-\frac{k(z+h)}{c_0})^2\ \phi_z]_z\ +\ N^2\phi = 0 \qquad (4.2)$$

This equation can be simplified using the transformation

$$g = \ln\ (1-\frac{k(z+h)}{c_0}) \qquad (4.3)$$

giving

$$\phi_{gg}\ +\ \phi_g\ +\ \frac{N^2}{k^2}\phi\ =\ 0 \qquad (4.4)$$

This is a linear homogeneous differential equation with solution

$$\phi(g)\ =\ e^{-g/2}(a_0\ \sin\ rg\ +\ b_0\ \cos\ rg\ ) \qquad (4.5)$$

$$\text{where } r = \sqrt{\frac{N^2}{k^2}-\frac{1}{4}} \qquad (4.6)$$

is the Richardson number.

We note that the solution is valid only for $|k|<2N$, where $k<0$ refers

to a velocity in the offshore direction and k>0 a velocity in the onshore direction. In the region of interest, starting from about 30 km seaward of North Rankin and extending to about 50 km inshore of it, the restriction on k corresponds to v(z)<2 m/s in the worst case. Observed values of shear velocity at North Rankin and Mooring 5 are all <0.15 m/s (Holloway 1987).

If we apply the boundary condition (2.15) at z=-h to (4.3) we find that $b_0=0$, giving

$$\phi(z) = a_0(1-\frac{k(z+h)}{c_0})^{-1/2} \sin[\ r\ \ln(1-\frac{k(z+h)}{c_0})\ ] \qquad (4.7)$$

The boundary condition (2.15) at z=0 gives

$$c_0 = -\frac{kh}{e^{n\pi/r}-1} \qquad (4.8)$$

where $n = \pm1,\pm2,\text{------}$ is the mode number

Values of $c_0>0$ represent the incoming tide, while $c_0<0$ represents the outgoing tide. When k<0 the incoming tide is represented by the mode n=1 while, for k>0, it is represented by the mode n=-1 (see figure 4.1). So $c_0(k)$ is a continuous function even though the parameter n is discontinuous at k=0. Here we are only considering the n=±1 modes because the observed tide has a single maximum with depth, and hence is a mode 1 wave. Higher modes will give increasing numbers of oscillations in the z profile. The modal function (4.7) is normalised so that $|\phi(z)_{max}| = 1$. This gives

$$a_0 = \frac{\sqrt{1+r^2}}{2r} \exp\ [\frac{\tan^{-1}(2r)}{2r}] \qquad (4.9)$$

Equations (2.16) and (2.22) can be evaluated with the modal function (4.7) to give

$$I = -\frac{\rho_0 a_0^2 k^2 h r^2 e^{-n\pi/r}}{c_0} \qquad (4.10)$$

$$\mu = \frac{2a_0 r e^{n\pi/r}(1-(-1)^n e^{-3n\pi/2r})}{h(r^2+9/4)} \qquad (4.11)$$

$$\delta = -\frac{kh^3 e^{n\pi/r}(e^{n\pi/r}+1)}{4(r^2+1)(e^{n\pi/r}-1)c_0^3} \qquad (4.12)$$

Using the bathymetry (3.23) we can solve (2.20) for t to find

$$t = \frac{1-e^{n\pi/r}}{kKh_0}\{ e^{\alpha\beta KX}-1\} \qquad (4.13)$$

We can then obtain solutions for (3.18) and the shock height (3.22), using (4.13) to eliminate t. It is found that

$$I_2(X) = -\frac{\alpha\beta(e^{n\pi/r}-1)}{(2+\alpha\beta)kh_0K}\{ e^{(2+\alpha\beta)KX}-1 \} \qquad (4.14)$$

and

$$\eta_1-\eta_2 = 2ae^{KX}\sin\psi \quad \phi(z) \qquad (4.15)$$

where ψ is defined implicitly by (3.16)

In (4.10) to (4.14) we use n=1 for k<0 and n=-1 for k>0, just as we did for (4.8). The values of I,μ,δ,t and $I_2(X)$ are then positive for all k.The breaking distance is the value of X when ψ=0, ie when

$$I_2(X) = \frac{1}{6AB} \qquad (4.16)$$

When the background current is against the phase speed of the internal tide we can expect a short breaking distance while, for a current with the internal tide, we can expect a longer breaking distance. This situation is mirrored in (4.12) because for k<0, the factor $(e^{\pi/r}-1)$ causes a rapid increase in $I_2(X)$, while for k>0 the factor $(1-e^{-\pi/r})$ gives a smaller rate of increase.

Validation trials

Before we can accept the numerical method we must show that the numerical solution is the same as the analytical solution in all respects for the linear background shear. This means that we need to compare numerical and analytical values of $c_0,\phi,\phi_z,I,\mu,\delta,t,\eta_1-\eta_2$ and breaking distance and to establish that errors are within some acceptable limits.

Accuracy of c_0 calculation

The numerical estimates of c_0 proved to be extremely accurate with the error ranging from 0.25% for 10 steps, to 0.15% for 80 steps. Since all of the other test variables depend on c_0, it is critically important that the error here is small. In figure 4.2 the analytical and numerical values of c_0 are compared as a function of distance up the shelf for k=-0.4. It can be seen that the agreement between the values is excellent.

Calculation of $\phi(z)$

The conjugate gradient algorithm is sensitive to the starting estimate. For some initial forms of $\phi(z)$ the algorithm will inevitably converge to the null solution (see Kammerer and Nashed,1972). Here a sinusoidal initial form is used as this produces nonzero solutions. Figure 4.3 shows a comparison between the analytical solution for $\phi(z)$ and the numerical solution at X=0 for k=-0.4. The agreement is good.

Accuracy of the calculated values of μ

A review of the numerical values of ϕ,ϕ_z,I,δ and μ during the trials revealed that μ was far less accurate than the other values. For

this reason it was decided to use the error in μ as the basis for selecting the convergence criterion. In each iteration we calculate the sum of the squares of the changes to the elements of the vector $\phi(z)$. For convergence this sum must be less than the criterion value. The results for 80 steps are shown in Table 4.1

Table 4.1

Errors in μ for various convergence criteria

Criterion	error in μ (%)
$<0.5\times10^{-6}$	45
$<0.3\times10^{-6}$	25
$<1.0\times10^{-7}$	9
$<0.7\times10^{-7}$	6
$<0.5\times10^{-7}$	4
$<0.3\times10^{-7}$	2
$<1.0\times10^{-8}$	1

Trials for 10,20 and 40 steps showed that the best value of the criterion was dependent on the number of steps. This raised the possibility that the accuracy of a particular value of the convergence criterion depended on the background velocity profile. This possibility had to be eliminated before the method could be used for background velocity profiles for which there are no analytical solutions for the modal function. To check the effect on convergence of a change in the profile of the background velocity, the above tests were repeated for different values of k. The results in each case were identical.

Accuracy of the other variables

For 80 steps the errors in the other important variables were small, as shown in Table 4.2.

Table 4.2

Errors in numerical estimates

variable	error(%)
I	0.5
δ	0.6
ϕ	0.5
$\eta_1-\eta_2$	1.7

Numerical values of c_0,ϕ,δ,μ,t and shock height are compared to the analytical values in figure 4.2 to figure 4.7. These values are for a linear background velocity profile with k=-0.4. The analytical solutions are graphed with the full line, while the numerical solutions are represented by the symbols. In order to maintain clarity only every eighth point in the numerical solution is plotted. In figure 4.7, the z dependence of the shock height is removed and the maximum value of the shock height $((\eta_1-\eta_2)/\phi(z))$, expressed in dimensional coordinates is plotted. The most dramatic evidence for the validity of the numerical solution comes from changing the value of k from -0.4 to +0.4 as this reverses the skew of $\phi(z)$. This is shown in figure 4.8. Note that the sign is also reversed, with $\phi(z)<0$ for $k>0$ but this is achieved by choice in order to fit the convention adopted in the analytical solution. The sign of

$\phi(z)$ is determined by an arbitrary multiplier but a change in the sign of $\phi(z)$ will cause a change in the sign of μ so that the sign of ξ is unaffected (see equation (2.21)).

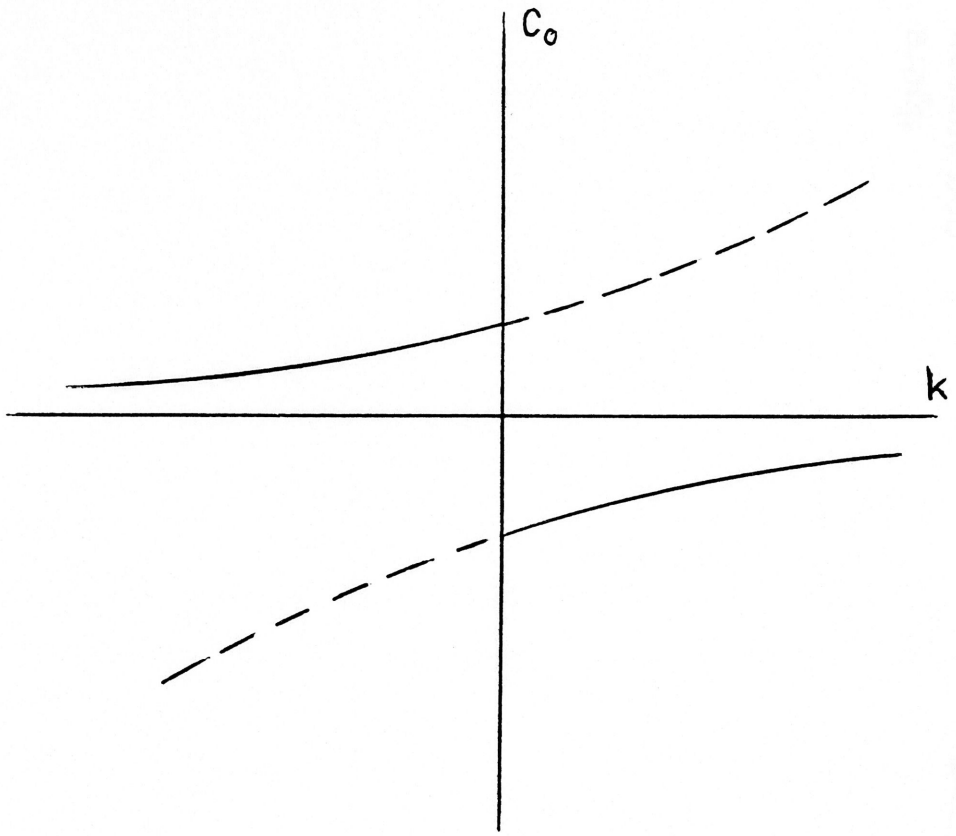

figure 4.1
graph of c_0 vs. k
mode n=1 denoted by full line
mode n=-1 denoted by dashed line

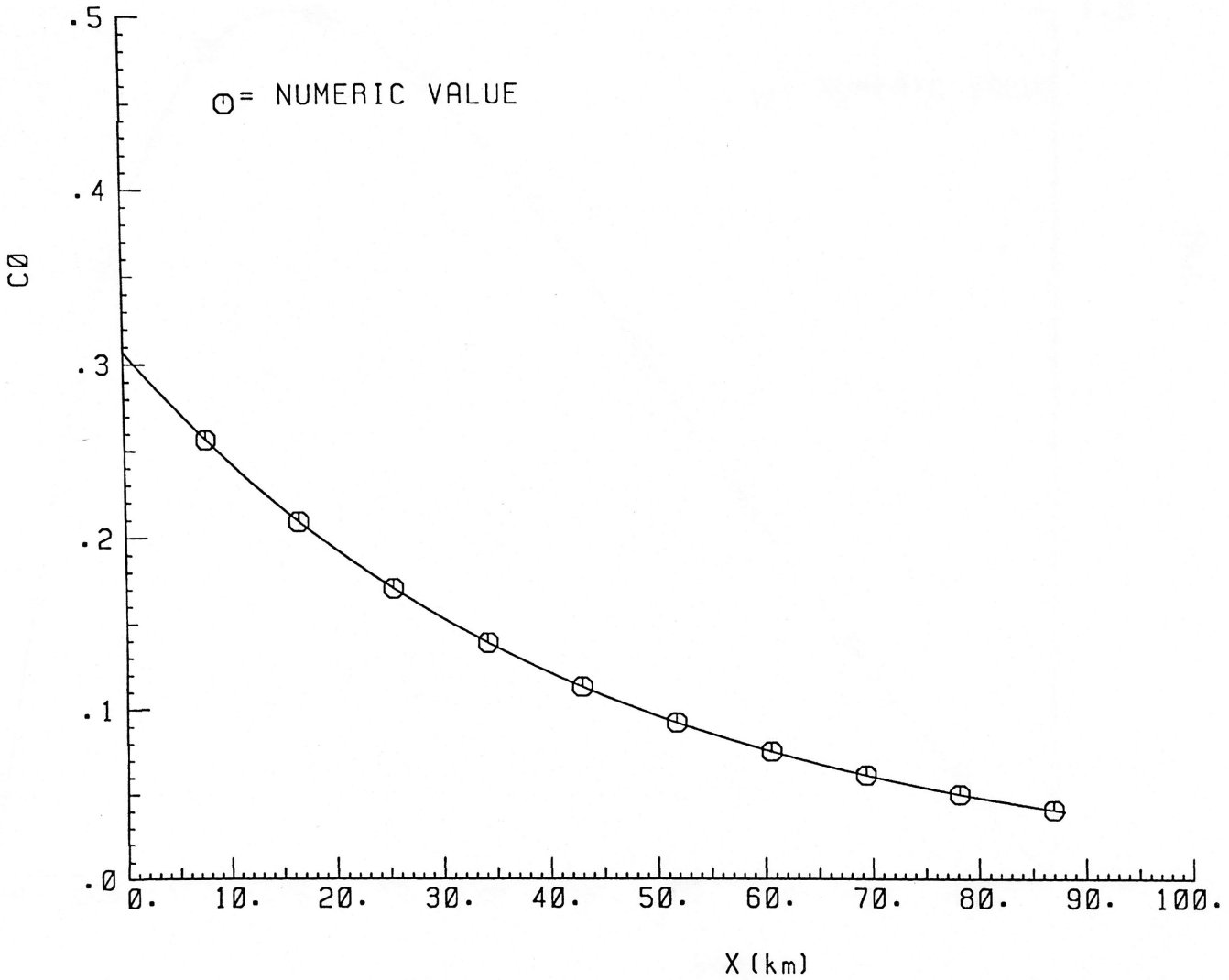

figure 4.2
comparison of analytical and numerical values for c_0 (for k=-0.4)

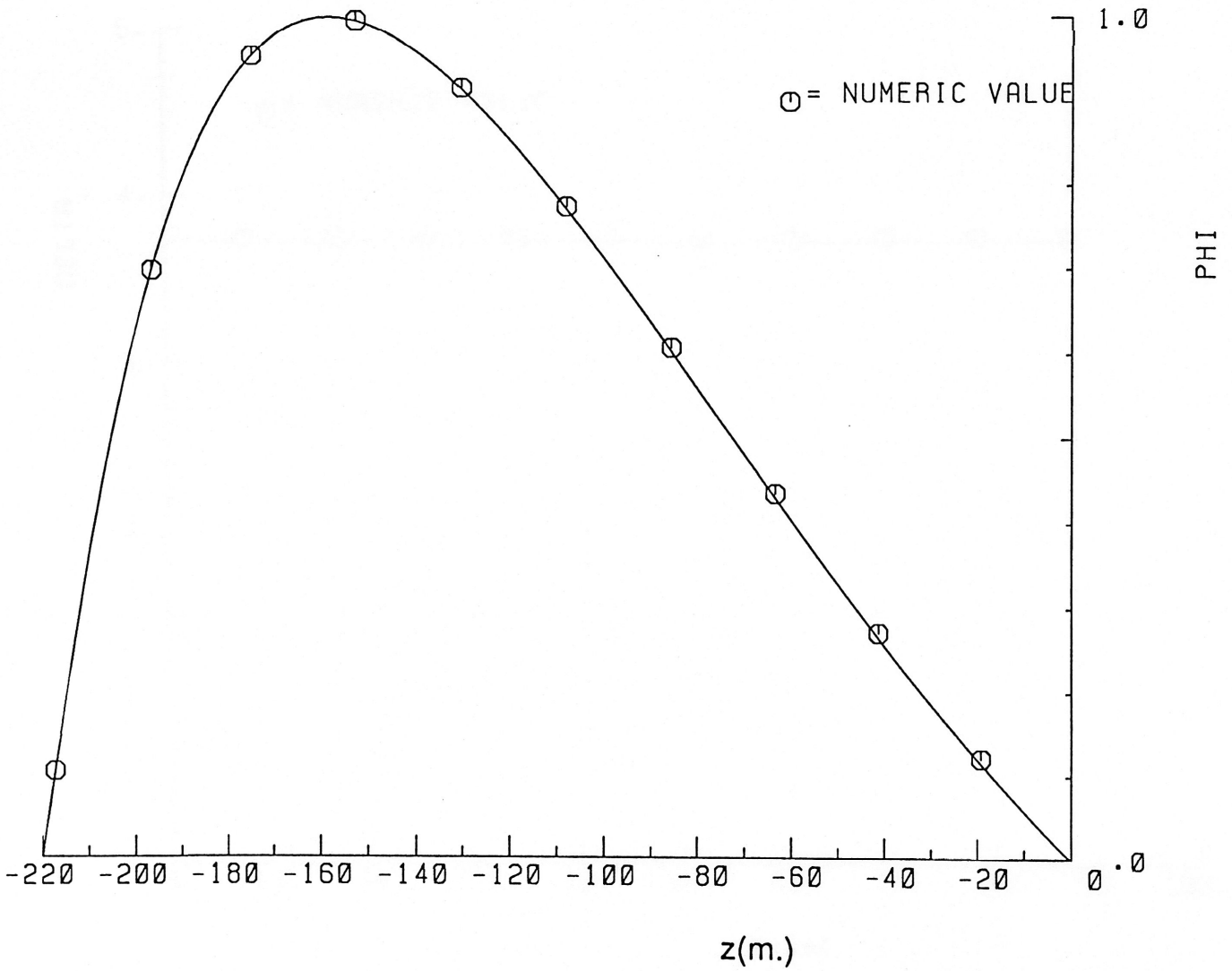

figure 4.3
comparison of analytical and numerical values for $\phi(z)$ at X=0 (for k=-0.4)

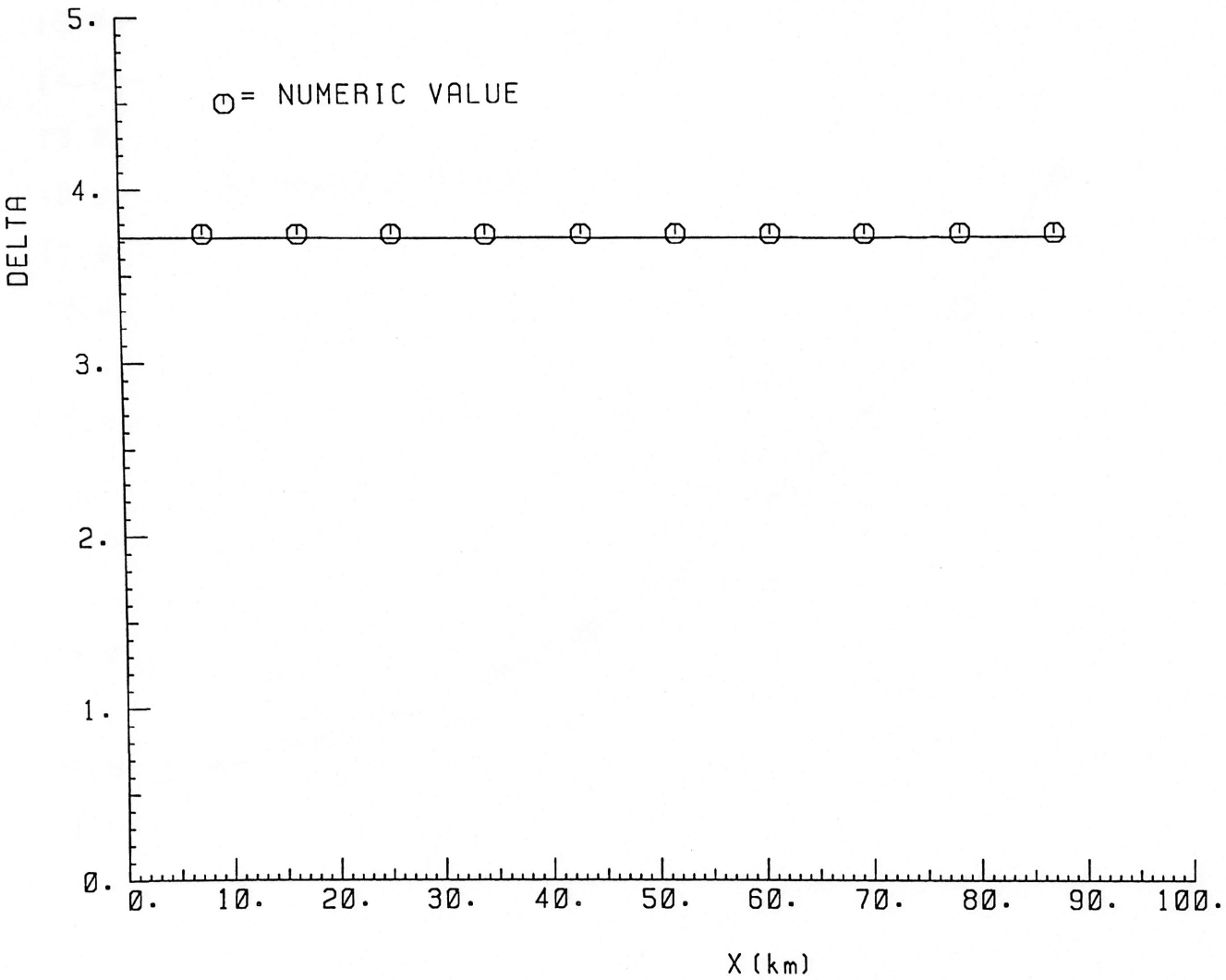

figure 4.4
comparison of analytical and numerical values for δ (for k=-0.4)

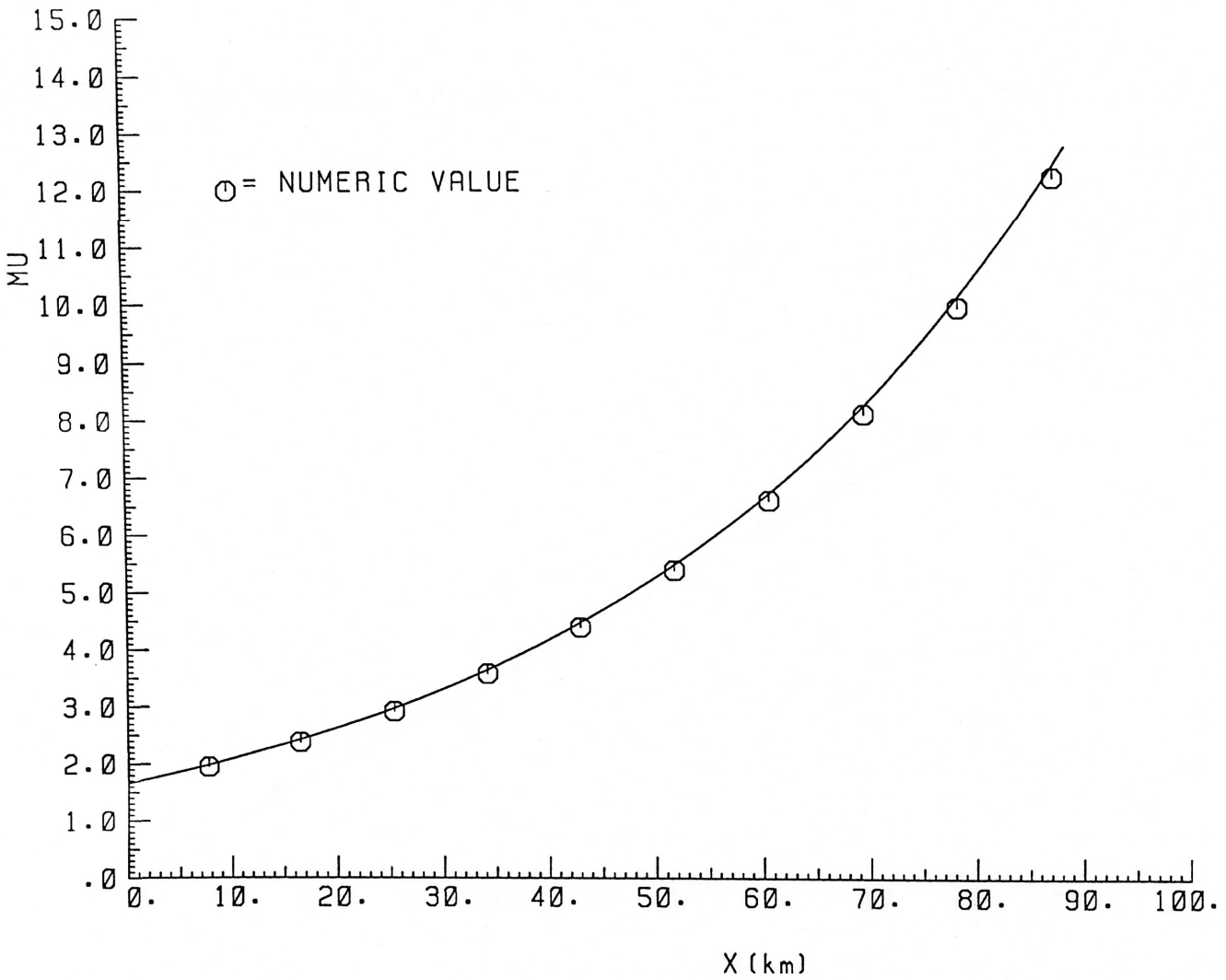

figure 4.5
comparison of analytical and numerical values for μ (for k=-0.4)

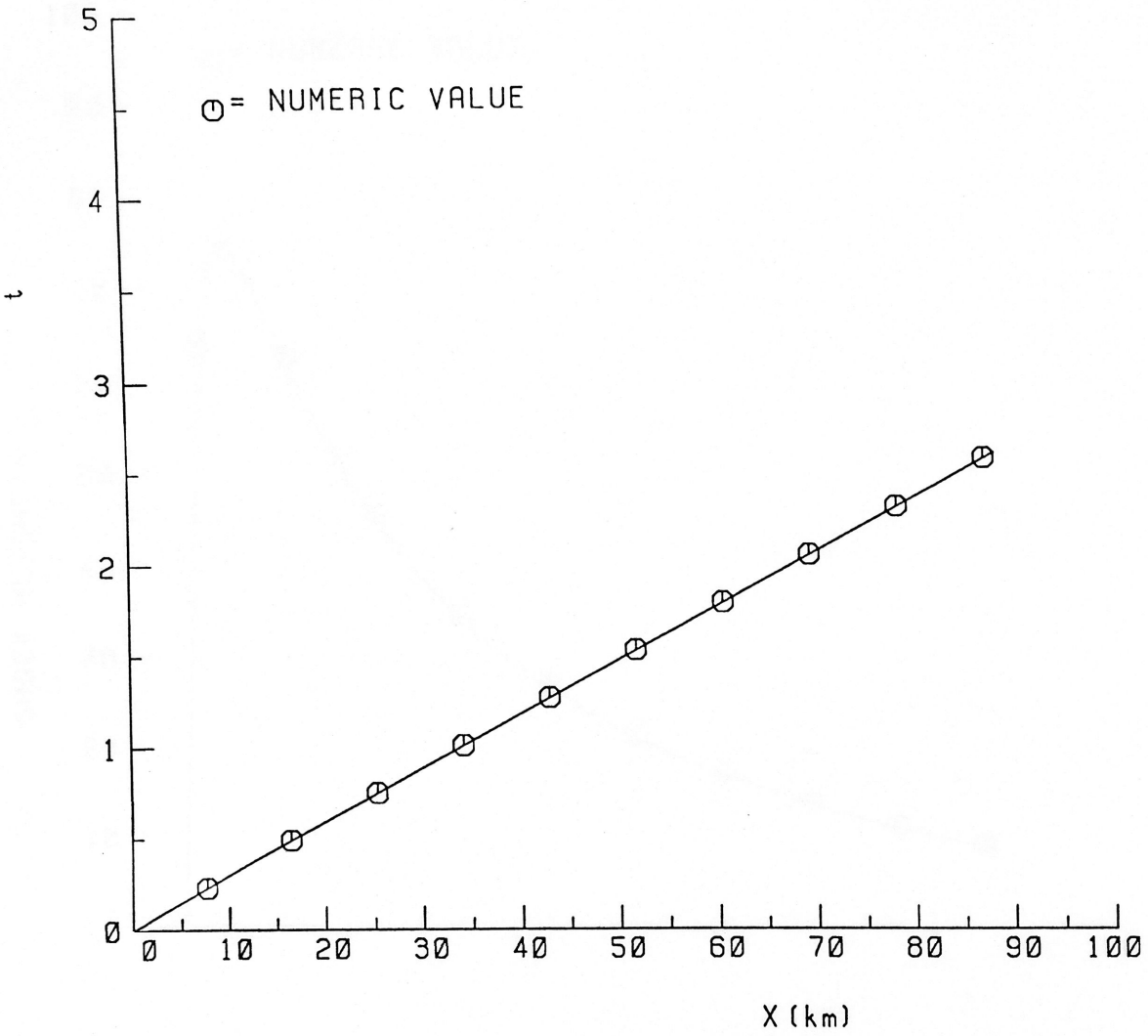

figure 4.6
comparison of analytical and numerical values for t (for k=-0.4)

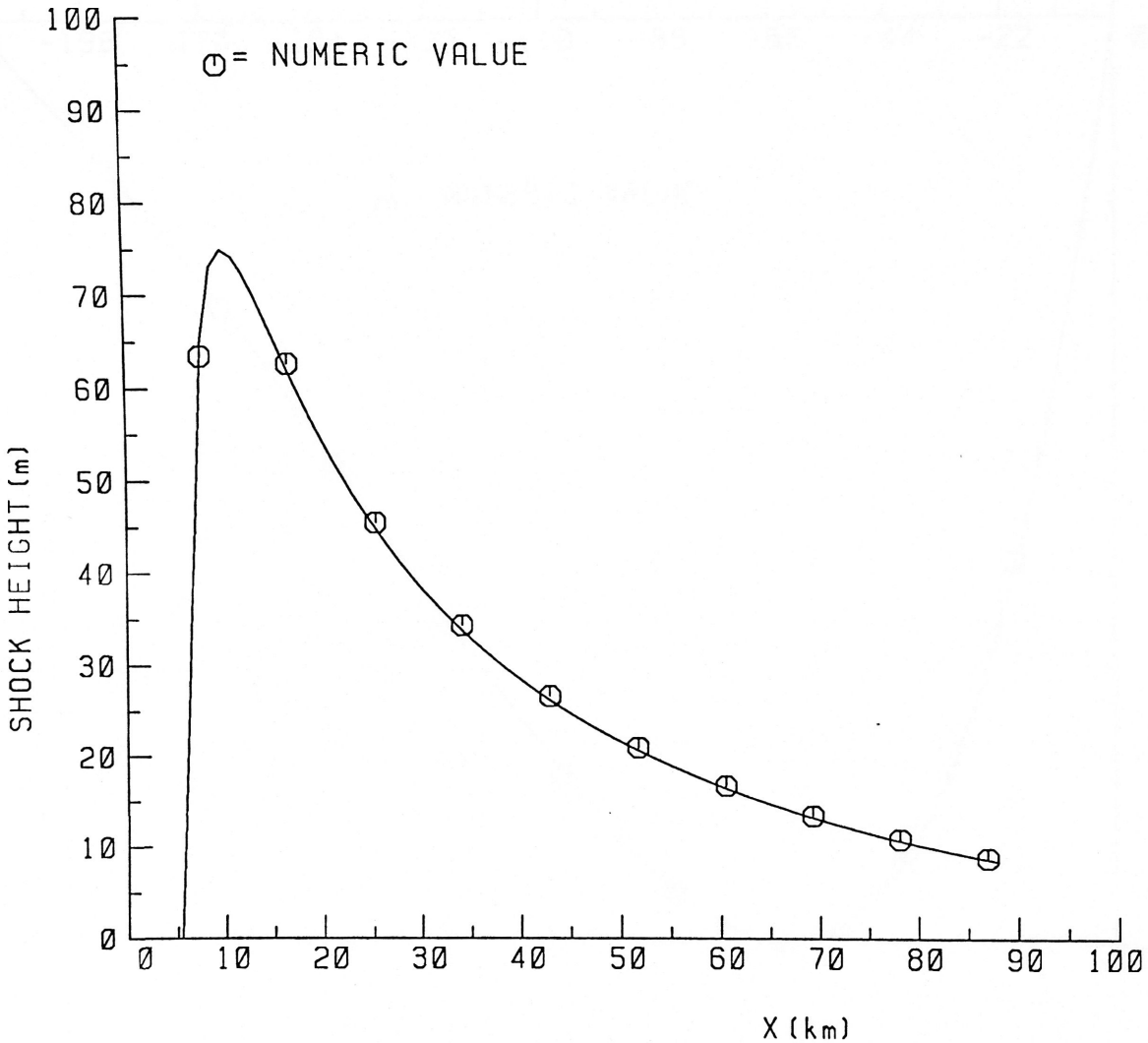

figure 4.7
comparison of analytical and numerical values for maximum shock height (for k=-0.4)

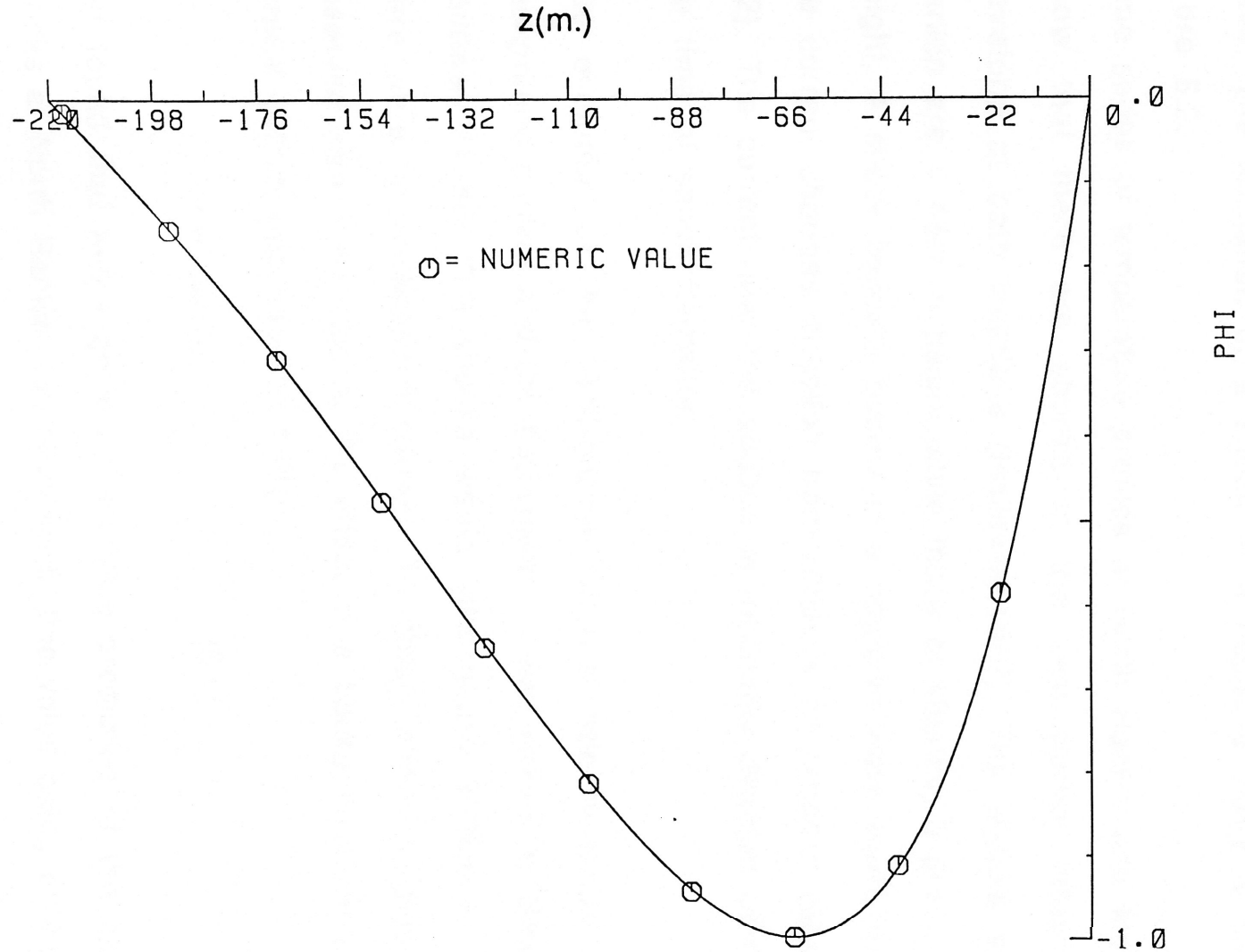

figure 4.8
comparison of analytical and numerical values for $\phi(z)$ at X=0 (for k= 0.4)

5. Comparison with observations

Internal waves described by the nonphysical amplitude u can form shocks only for a jump up in u. The variable u is positive behind the shock and thus this type of wave will be known as a positive wave throughout this discussion. The formation of a shock in a u wave is shown in figure 5.1. Waves described by the physical amplitude η can form shocks regardless of the sign of η behind the shock. When $\eta<0$ behind the shock the wave will be described as a negative wave. The formation of a shock in a negative wave is shown in figure 5.2.

Time series of temperature profiles at North Rankin and Mooring 5 show that there are shocks in the semi-diurnal internal tide waveform at both locations (Holloway,1987). The shocks at North Rankin are ~ 45m in height while those at Mooring 5 are ~ 20m in height. A shock typically occurs in a negative wave ($\eta<0$) just after the current changes direction from offshore to onshore (see figure 1.2). The current near the seabed is invariably directed offshore at the time of shock formation.

The evolution of the semi-diurnal internal tide depends on the background current and the bathymetry. It was shown by Smyth and Holloway (1988) that shocks would take nearly 300km to form if there were no background current. To obtain shock heights of the observed size, they studied the effect of a background linear shear current (which opposes the tide)

$$v = -k(z+h) \qquad (5.1)$$

and found that k=0.4 gave an accurate prediction of the observed shocks at North Rankin and Mooring 5, this value being of the same

order as the observed shears. Smyth and Holloway also found that neither the value of the initial amplitude nor the location of the starting point of the tide made any significant difference to the predicted shock heights at North Rankin and Mooring 5.

Since the background current is the critical factor in the formation of the shocks, we need to determine the size and direction of this current and study the effect of this more realistic current profile. The observed current is a combination of the semi-diurnal internal tide and the background current and there is no time when the observed current is free from tidal influence. So the background current cannot be measured directly. Holloway (1987) calculated 24-hour averaged currents for each measuring point (figure 1.3). These averaged currents are the only information we have about the background current, but they show a distinctly nonlinear profile.

If we assume that v(z) varies only slowly with time (ie on a timescale >> 24 hours) then

$$\text{av. current} = v(z) + \frac{\Delta c_0}{2} \qquad (5.2)$$

where Δc_0 is the difference between the linear wavespeeds for the incoming and outgoing tides. The averaged profile would have the same shape as the background profile but would be translated from it. Even with this information, we still know little about the background profile. At North Rankin the current was measured at four different depths, which provides little definition of the profile while at Mooring 5, the current was measured at three different depths, which gives even less definition. In addition the

profiles at these locations give the only information as to how the background profile varies in the onshore direction.

As a first approximation, the current profile was taken to be very smooth, for example the parabola

$$v = -0.52456(z/h)^2 - 0.61456(z/h) - 0.09 \qquad (5.3)$$

A comparison between this profile and the observed current at the four depths at North Rankin is shown in figure 5.3. These curves gave breaking distances of 53-55 km, predicting no shock at North Rankin and a very large (~ 200m) shock at Mooring 5. The curved profiles were then replaced by a piece-wise linear profile where each pair of average currents is connected by a straight line and the top line is extrapolated to the surface. This profile is shown in figure 5.4 and is defined in non-dimensionalised coordinates by

$$v = \begin{cases} -0.5(z + 0.3h) & z \geq -0.5h \\ 0.2(z + h) & z < -0.5h \end{cases} \qquad (5.4)$$

This resulted in a breaking distance and shock height very similar to those of the curved profiles. Since parabolic and piece-wise linear profiles give very similar results, piece-wise linear profiles will be used from now on for simplicity.

For this unsuccessful profile, the major change in slope occurred at the second measured point (depth = 53m for North Rankin). The effect of moving this point of maximum slope closer to the top point (depth = 23m) will now be investigated. This results in the shear in the upper part of the current being increased. For a sufficiently large slope $(\frac{dv}{dz})$, this type of profile was able to give

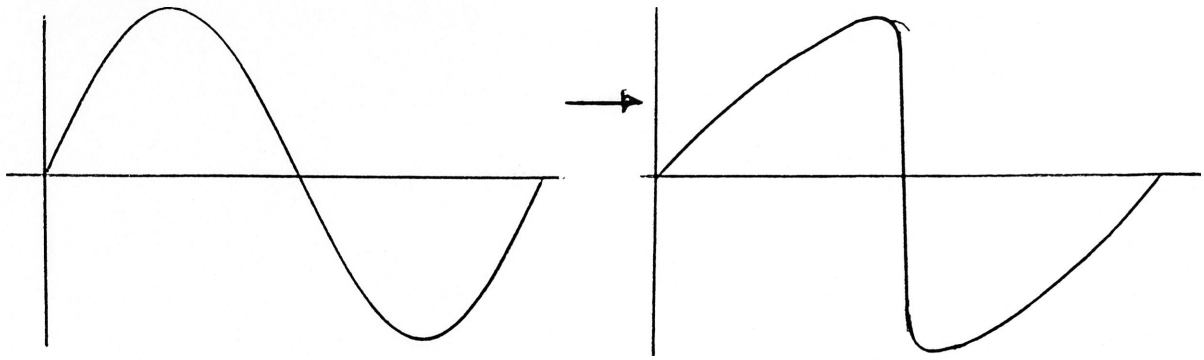

figure 5.1
formation of a shock in a positive wave
(upward hydraulic jump)

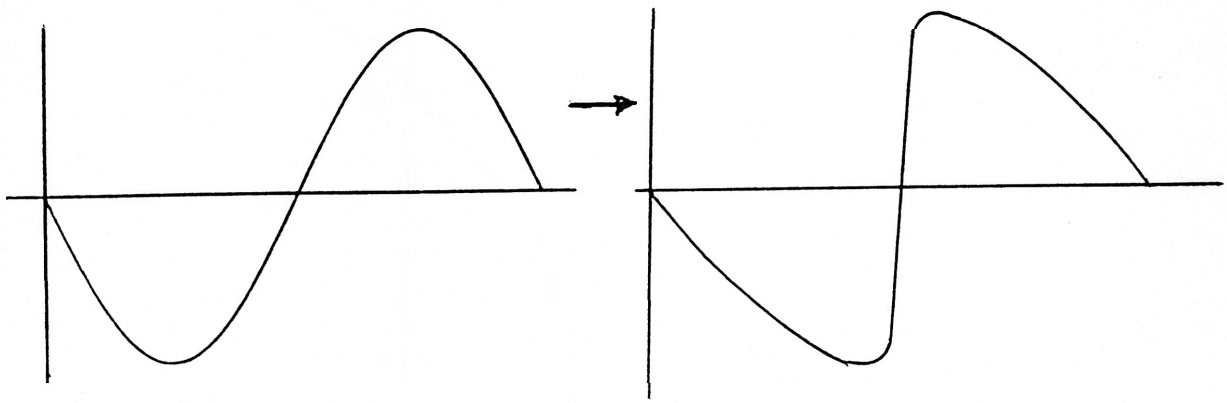

figure 5.2
formation of a shock in a negative wave
(downward hydraulic jump)

figure 5.3
parabolic profile

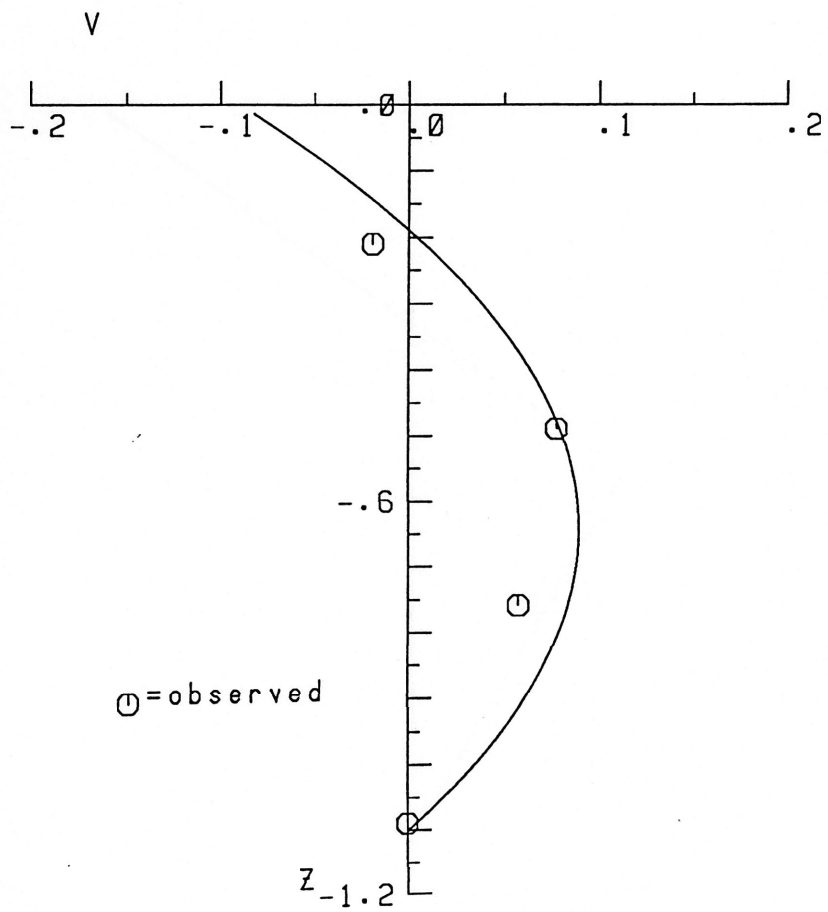

figure 5.4
piecewise linear profile

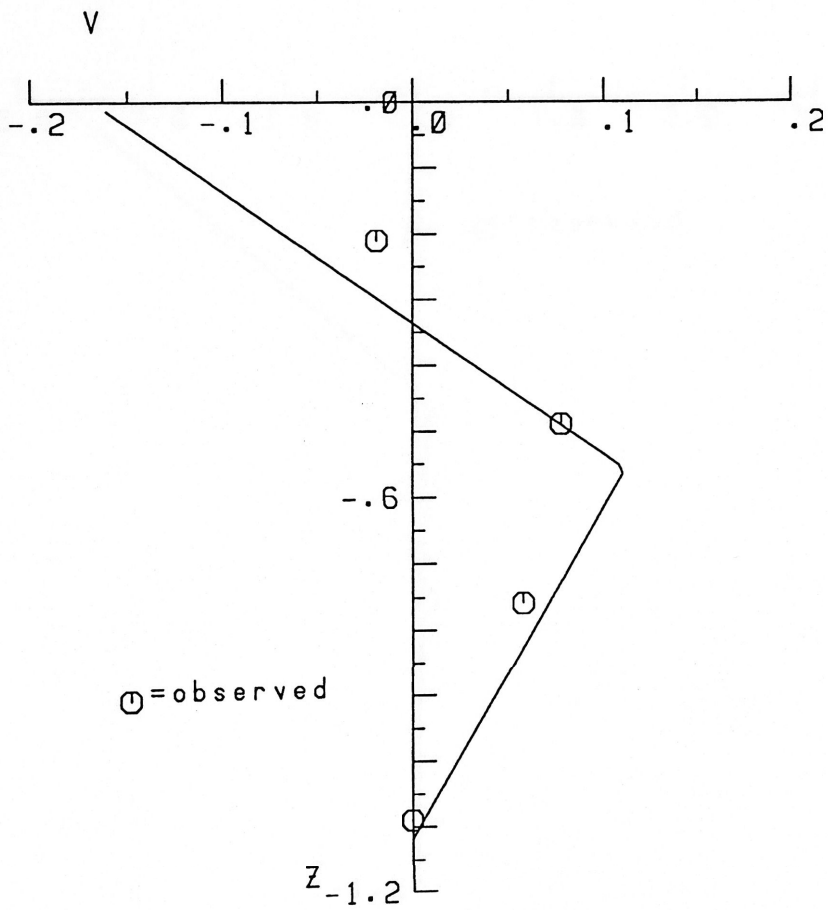

figure 5.5
profile with large shear near surface

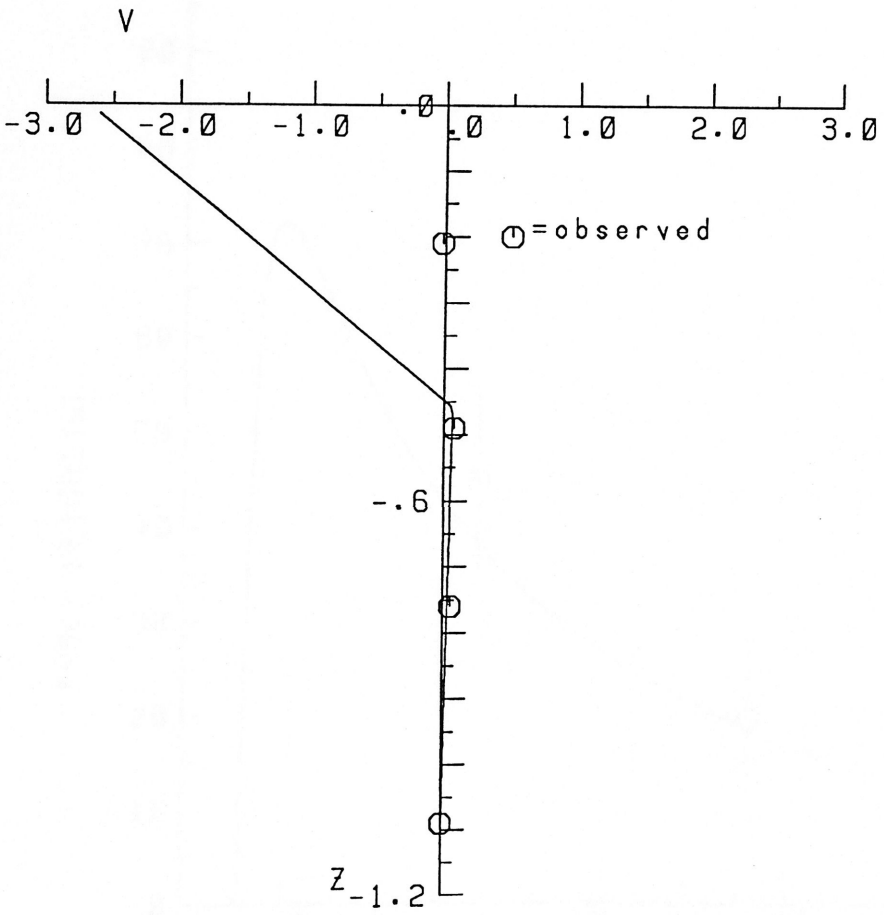

figure 5.6
shock heights caused by profile in figure 5.5

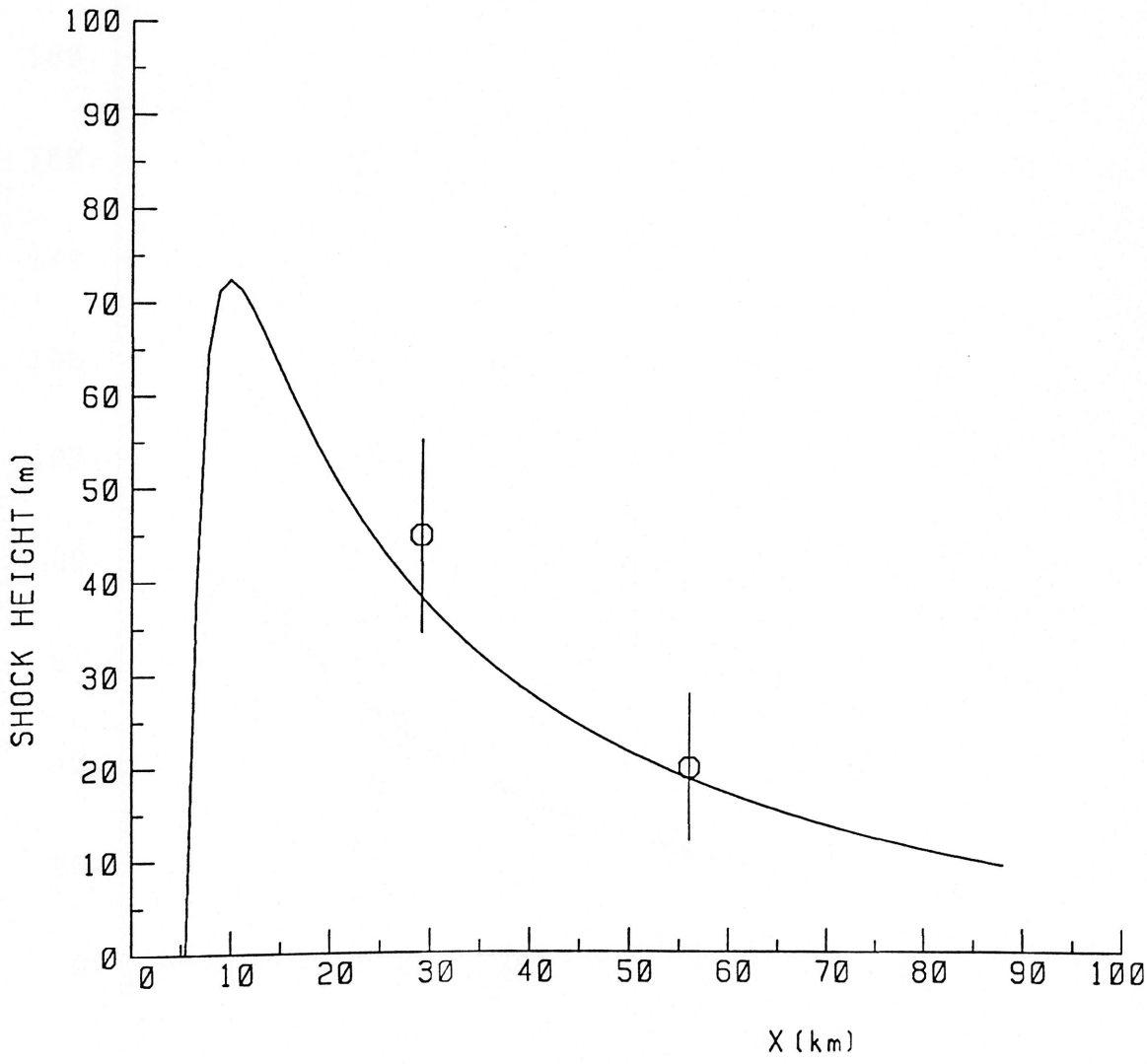

figure 5.7
shock heights for k = +1.4

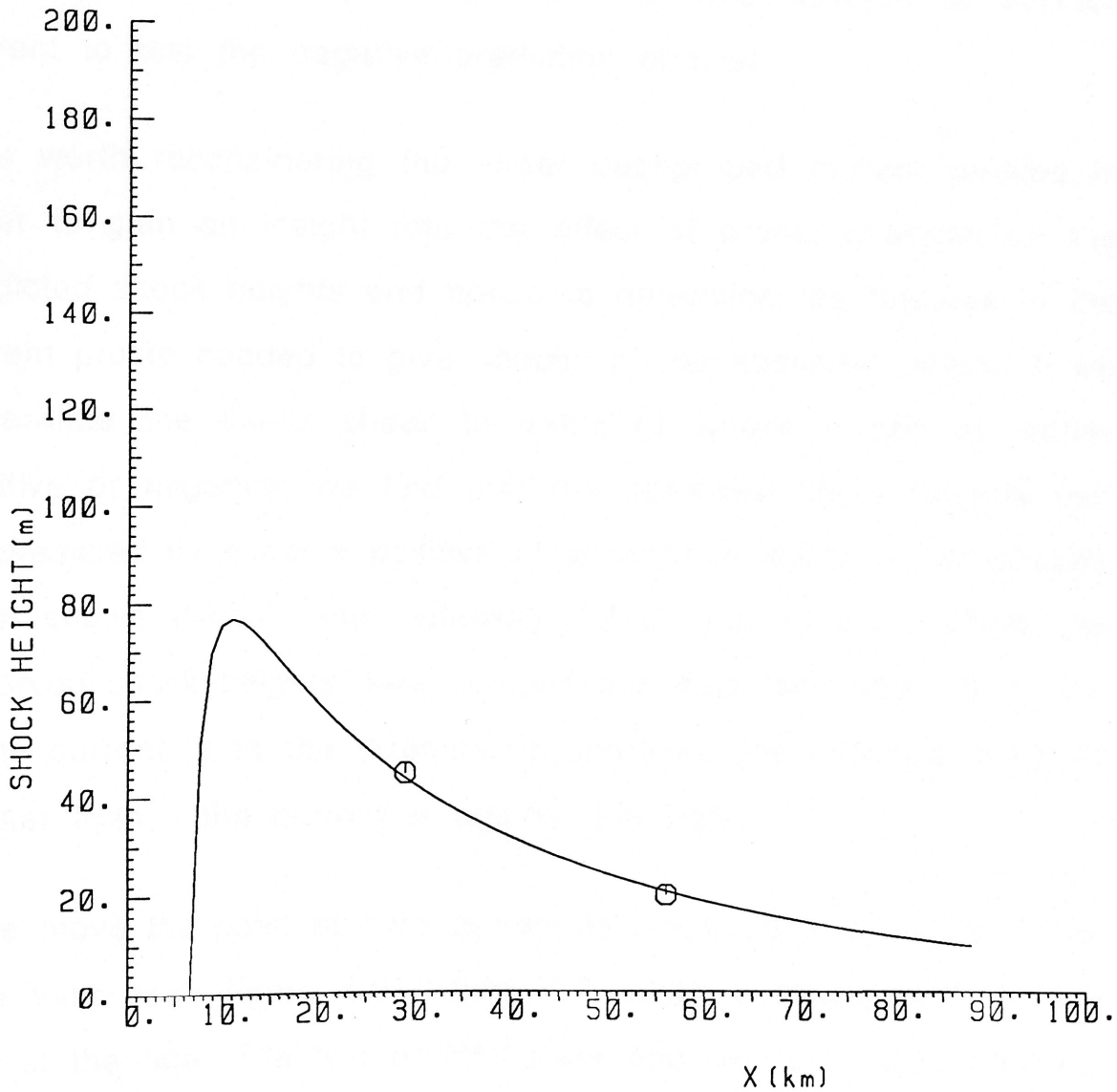

shocks of the observed sizes. For the case

$$v = \begin{cases} -6.0(z + 0.4h) & z \geq -0.41h \\ 0.1(z + h) & z < -0.41h \end{cases} \qquad (5.5)$$

(see figure 5.5), the resulting shock heights are shown in figure 5.6. These profiles also predict $\eta<0$, giving a negative wave, which is in accordance with the observations. However, when the tide is taken into account, they predict a positive current at the seabed and a strong negative current at the surface. The positive current at the seabed is the opposite to the observed current at the time of formation of the shock. There are no observations of surface current to test the negative prediction against.

It is worth reconsidering the linear background current profiles in order to gain an insight into the effect of profile changes on the predicted shock heights and hence to determine the features in the current profile needed to give shocks of the observed height. If we generalise the linear shear to $v=k(z+h)$ where k can be either positive or negative, we find that the observed shock heights can be predicted by either a positive or a negative shear. It has already been shown (Smyth and Holloway, 1988) that $k=-0.4$ predicts the observed shock heights; $k=+1.4$ does this also (see figure 5.7). So, if the current is in the direction of the tide, the required shear is greater than if the current is against the tide.

If we move the point of zero current to the surface by adopting the form $v=kz$ (see figure 5.8), then $k>0$ gives a background current against the tide. The two profiles $v=kz$ and $v=-k(z+h)$ give identical breaking distance and shock height predictions, but when $v=kz$, then

$\eta<0$ so that the wave is negative and when $v=-k(z+h)$, then $\eta>0$ so that the wave is positive. We have already seen that a strong negative shear near the surface gives $\eta<0$ so we cannot generalise, at this stage, about the effect of k on the sign of η. We are looking for a background current which

(i) is against the tide, so that the shear required to give shocks of the observed heights is less (and of the same order as the observed shears)

(ii) gives $\eta<0$

and (iii) gives negative flow at the seabed.

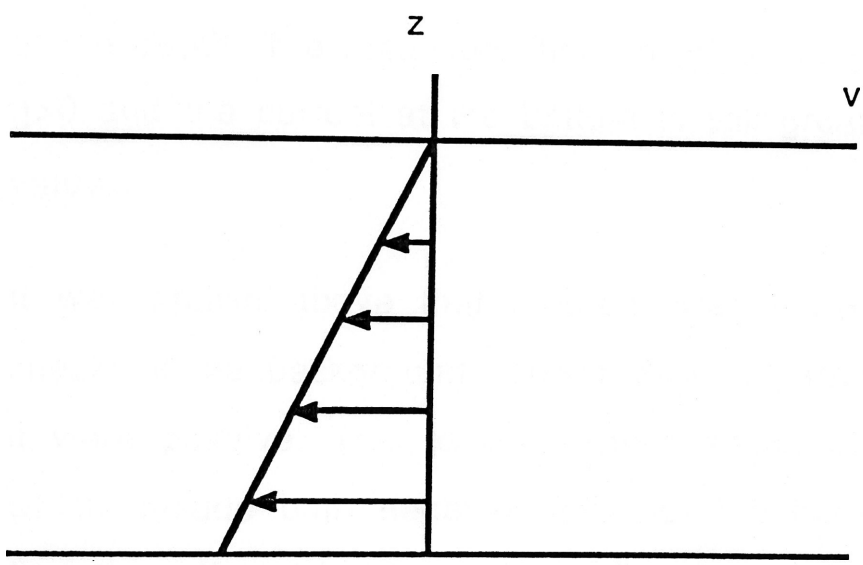

figure 5.8

background current profile for v=kz

The observations of currents (figure 1.2) show that, at each shock the current at the seabed is strongly against the tide. Changes in the current at the seabed are out of phase with changes at other points, indicating that changes in v(z) at the bottom could occur on a tidal timescale. If the current at the bottom was generated by

the tide but was against both the incoming and outgoing tide, the average over the incoming and outgoing tide could still be zero, as the averaged currents show. Current profiles with a strong negative shear at the bottom also predict the observed shock heights. In fact a profile v(z) and its mirror image v(z+h) will give identical shock height curves. Two profiles with a strong negative shear at the bottom are shown in figures 5.9 and 5.10, along with their predicted shock heights. In both cases the current near the bottom is strongly negative but $\eta>0$, indicating a positive wave. The size of the negative current is much greater than the observed value, but a comparison of figures 5.9 and 5.10 shows that the slope of the shear can be reduced if it acts over a greater fraction of the depth. The predicted shock heights are good but we still have $\eta>0$ and the current at the bottom is still greater than the observed value.

It was shown above that a shear was more effective in forming shocks if the background current were negative than it would be if it were positive. This loss of effectiveness is also true of shears which include both negative and positive background currents. To find the effect of this on a nonlinear profile, the following profile was used

$$v = \begin{cases} -0.1(z+0.4h) & z \geq -0.4h \\ 3.0(z+0.4h) & z < -0.4h \end{cases} \qquad (5.6)$$

For this profile, $v=0$ at $z=-0.4h$ and $v<0$ for all other values of z. The result of removing all positive background currents was a reduced breaking distance of 4.36 km and reduced shock heights, substantially lower than the observed values. The profile and its

shock height curve are shown in figure 5.11. Since $\eta>0$ this profile also predicts a positive wave.

We shall now change the slope of the upper portion of the current profile to reflect the slope between the top two average currents (23m and 53m depth). That is

$$v = \begin{cases} -0.5(z+0.4h) & z \geq -0.4h \\ 3.0(z+0.4h) & z < -0.4h \end{cases} \qquad (5.7)$$

The increased shear near the surface reduces the breaking distance to only 1.16km and gives extremely small shock heights.

To reduce the maximum current at the seabed, we shall reduce the slope at the bottom of the profile. For a profile

$$v = \begin{cases} -0.5(z+0.4h) & z \geq -0.4h \\ 2.0(z+0.4h) & z < -0.4h \end{cases} \qquad (5.8)$$

the breaking distance is 17.2km and the shock heights are twice the observed values, indicating that a large shear is necessary at either the bottom or the top in order to produce the observed shock heights. In addition, the predicted linear wave speed is quite low ($c_{0\ max}$= 16 cm/s) which leads to a substantial negative current at a depth of 23m,which is contrary to observations.

The depth at which v=0 is now lowered from z=-0.4h to z=-0.6h and the profile

$$v = \begin{cases} -0.5(z+0.6h) & z \geq -0.6h \\ 3.0(z+0.6h) & z < -0.6h \end{cases} \qquad (5.9)$$

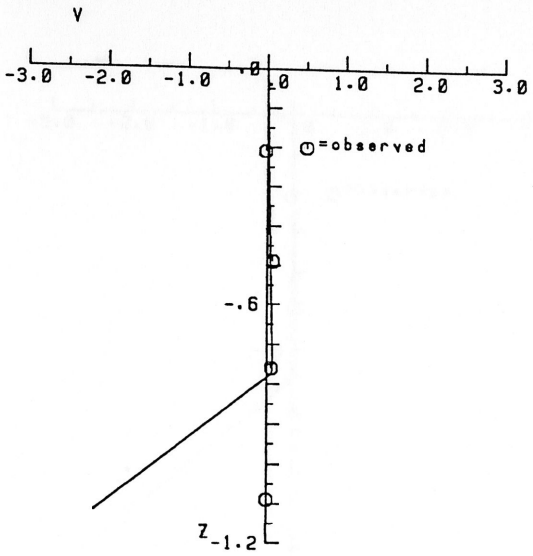

figure 5.9
profile with strong shear near seabed
and associated shock curve

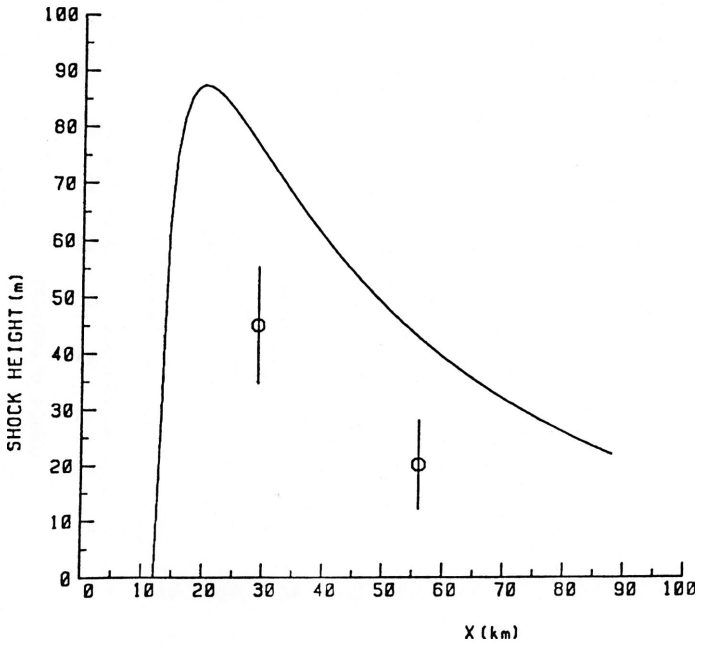

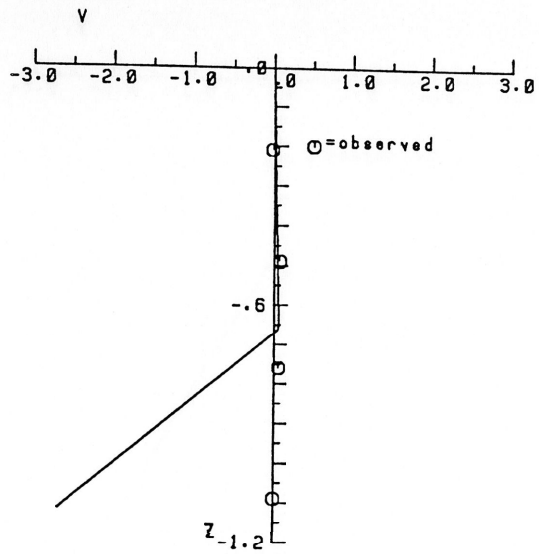

figure 5.10
profile like figure 5.9 with shear near seabed active over a larger fraction of depth

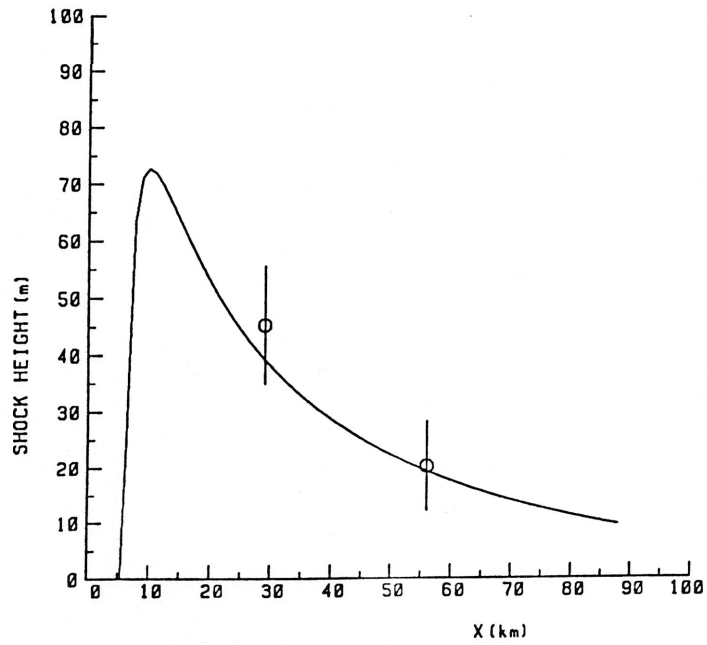

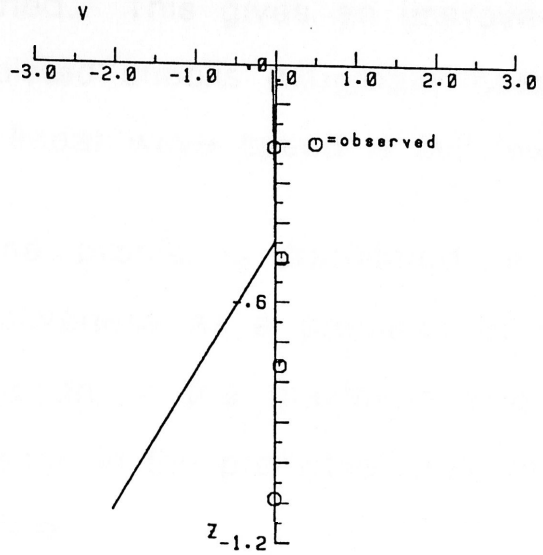

figure 5.11
profile with no positive currents
and its associated shock curve

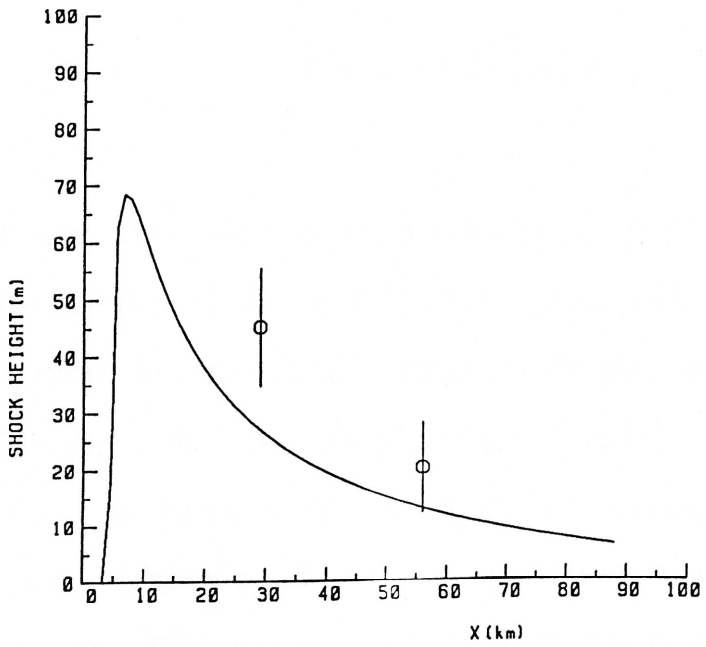

is tried. This gives an improved breaking distance of 9.7km and predicted shocks marginally outside the accepted range. However the linear wave speed is still low

If the profile is translated in the direction of positive v, its effectiveness as a producer of shocks is reduced but we gain a reduction in the maximum negative background current and an increase in the predicted linear wave speed. Hence we consider the profile

$$v = \begin{cases} -0.5(z+0.4h) & z \geq -0.5714h \\ 3.0(z+0.6h) & z < -0.5714h \end{cases} \qquad (5.10)$$

This results in a similar breaking distance (9.4km) and shock evolution to the previous profile (see figure 5.12) with the maximum linear wave speed being raised from 16 cm/s to 45 cm/s.

All of the profiles with a large shear at the seabed predicted $\eta>0$. This can be explained as follows. From (2.21) sign(η) =sign(μ), all of the other terms being positive. To calculate μ we evaluate

$$\int_{-h}^{0} \rho_0 (c_0-v)^2 \phi_z^3(z) dz \qquad (5.11)$$

If we consider the modal function $\phi(z)$ (see figure 4.3) we see that the slope $\phi_z(z)$ is negative near z=0 and is positive near z=-h. Putting a large shear near z=-h causes the region where $\phi_z>0$ to dominate in the integral (5.11) for μ, thus ensuring that $\mu>0$. In order to have $\mu<0$, we need to increase the weight given to the region where $\phi_z<0$. That is we need a large negative shear near the surface. We have seen that a background current profile with a

strong negative current near the surface gives both a negative wave and shocks of the observed heights. An additional current which is generated by the tide and opposes the tide but which is confined to the bottom 10% of the depth will cause only a slight reduction in the effectiveness of shock formation and would explain the negative flow at the seabed. We check the truth of this by using the composite profile

$$v = \begin{cases} -5(z + 0.35h) & z \geq -0.36h \\ 0.2(z + 0.55h) & -0.92h \leq z < -0.36h \\ 3(z + 0.9h) & z < -0.92h \end{cases} \qquad (5.12)$$

This profile and its shock height curve are shown in figure 5.13.

Conclusions

The evolution of the semi-diurnal internal tide is controlled by the slope of the background current profile (the shear) and by the direction of the current. When the slope is zero, shocks are absent. For a slope k, an increase in |k| causes an increase in the rate of evolution of the internal tide.

The formation of shocks in the internal tide could be caused either by a shear in a positive background current, or by a shear associated with a negative background current, or by a shear associated with a current which is positive or negative depending on the depth, but the shear required for a positive current is three times the size of the shear required for a negative current.

The shape of the background current profile must be compatible with the 24-hour averaged current profiles at both North Rankin and Mooring 5.

The evolution of shocks in the internal tide on the North West Shelf is associated with a background current profile which has both positive and negative currents, but the greatest slope in the profile occurs with a strong negative current.

The observed values of shock height can be caused by a strong shear associated with a negative current either near the surface or near the seabed. However, while a negative current and strong shear near the surface is compatible with the profile of averaged currents, a negative current and strong shear near the seabed is not. When the negative current near the seabed is a product of the tide rather than a true background current, the result will be compatible with the profile of averaged currents.

When the shear near the surface dominates, the shock will form in a negative wave, while the shock forms in a positive wave for a dominant shear near the seabed. This corroborates the finding of Holloway(1987) who used a two layer hydraulic model and found that when the flow near the surface became hydraulically supercritical a downward hydraulic jump would occur, while a supercritical flow near the seabed gave an upward hydraulic jump.

A typical shock at North Rankin forms in a negative wave (ie is a downward hydraulic jump) so the shear near the surface must dominate in the typical case.

In order to get numerical results which agree with the observations of shock heights at North Rankin and Mooring 5, we need to include a strong shear near the surface in the background current profile. This indicates a negative current of more than 2m/s. at the surface which is not compatible with observed values of tidal currents of ~0.5m/s. However we know nothing about the evolution of the background current as we move up the shelf.

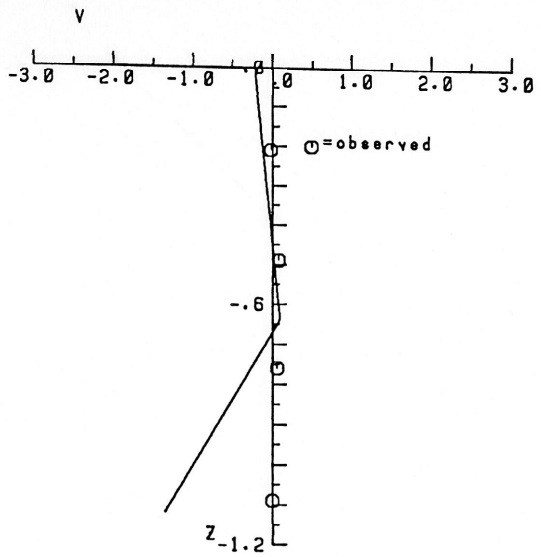

figure 5.12
shock curve for profile with some positive currents and with the major shear acting over less than half the depth

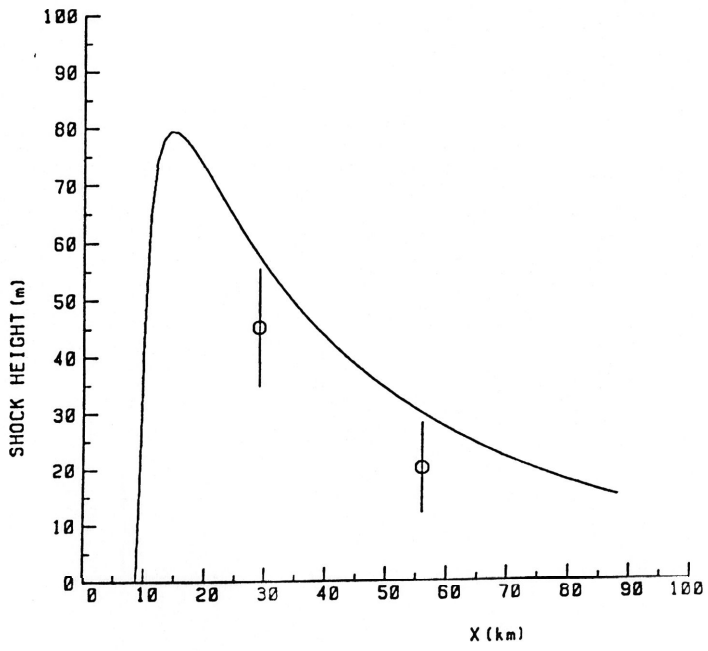

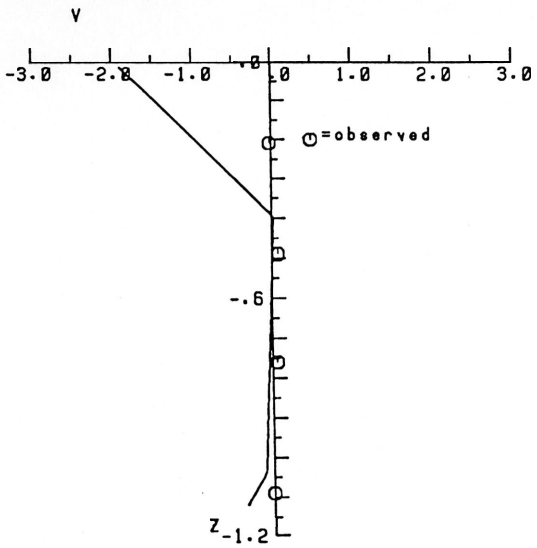

figure 5.13
shock height curve for composite profile
with strong shears near both the surface
and the seabed

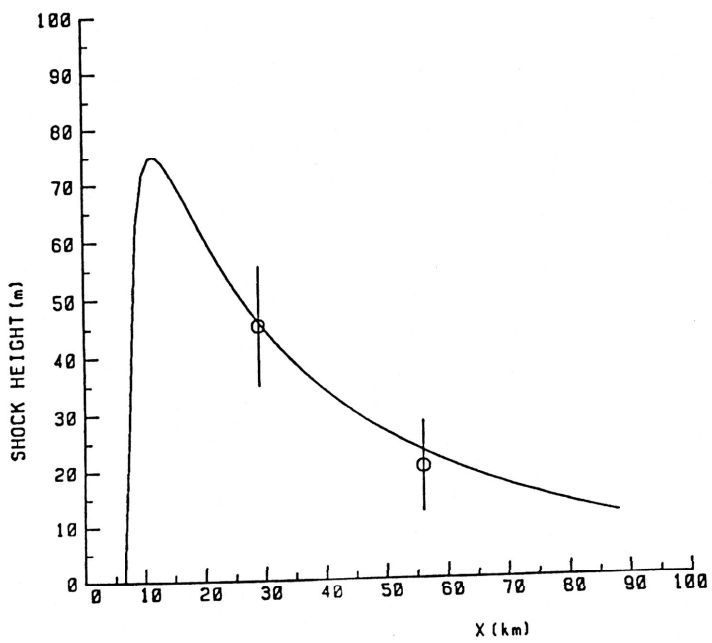

References

Gear, J.A. and Grimshaw, R., 1983, "A second order theory for solitary waves in shallow fluids", Phys. Fluids.,26(1),pp14-29.

Grimshaw, R., 1984, "Solitary waves in density stratified fluids" in "Nonlinear Deformation Waves",ed. U. Nigel and J. Engelbrecht, Springer Verlag, New York.

Holloway, P.E., 1987, "Internal hydraulic jumps and solitons at a shelf-break region on the Australian North West Shelf", J. Geophys. Res., 92(C5), pp 5405-5416.

Holloway, P.E. and Nye,H.C., 1985, "Leeuwin current and wind distributions on the southern part of the Australian North West Shelf between January 1982 and July 1983", Aust. J. Mar. Freshw. Res., 36, pp 123-137.

Kammerer, W.J. and Nashed, M.Z., 1972, "On the convergence of the conjugate gradient method for singular linear operator equations", SIAM J. Numer. Anal. 9(1), pp 165-181.

Smyth, N.F. and Holloway, P.E., 1988, "Hydraulic jump and undular bore formation on a shelf break", J. Phys. Ocean. 18(7) pp 947-962.